

Oskarshamn site investigation

Groundwater flow measurements and SWIW tests in boreholes KLX02 and KSH02

Erik Gustafsson, Rune Nordqvist
Geosigma AB

May 2005

Svensk Kärnbränslehantering AB

Swedish Nuclear Fuel
and Waste Management Co
Box 5864
SE-102 40 Stockholm Sweden
Tel 08-459 84 00
+46 8 459 84 00
Fax 08-661 57 19
+46 8 661 57 19



Oskarshamn site investigation

Groundwater flow measurements and SWIW tests in boreholes KLX02 and KSH02

Erik Gustafsson, Rune Nordqvist
Geosigma AB

May 2005

Keywords: Laxemar, Simpevarp, Hydrogeology, Borehole, Groundwater, Flow, Tracer tests, Dilution probe, SWIW test.

This report concerns a study which was conducted for SKB. The conclusions and viewpoints presented in the report are those of the authors and do not necessarily coincide with those of the client.

A pdf version of this document can be downloaded from www.skb.se

Abstract

This report describes the performance, evaluation and interpretation of *in-situ* groundwater flow measurements and single well injection withdrawal tracer tests (SWIW-tests) at Laxemar and Simpevarp areas at the Oskarshamn site. The objective of the activity was to determine the groundwater flow in selected fractures/fracture zones intersecting the cored boreholes KLX02 and KSH02. The objective was also to determine radio nuclide transport properties in a single fracture and a fracture zone by means of SWIW-tests in borehole KSH02. The borehole dilution probe was also used for water sampling (class 5) in a single fracture at 957 m depth in borehole KSH02. The result of the chemical analysis is reported elsewhere and not included in this report.

Groundwater flow measurements were carried out in 4 single fractures and 3 fracture zones at depth ranging from 176 to 957 m. Hydraulic transmissivity ranged within $T = 1.3 \times 10^{-8} - 7.4 \times 10^{-6} \text{ m}^2/\text{s}$. The results of the dilution measurements in boreholes KSH02 and KLX02 show that the groundwater flow varies considerably in fractures and fracture zones during natural undisturbed conditions, nevertheless the general trend is that flow rates and Darcy velocities decreases with depth. Flow rate ranged from 0.09 to 2.81 ml/min and Darcy velocity from 3.4×10^{-9} to $1.0 \times 10^{-7} \text{ m/s}$ ($2.9 \times 10^{-4} - 8.6 \times 10^{-3} \text{ m/d}$) which are within the range that can be expected out of experience from previously performed dilution measurements under natural gradient conditions at other sites in Swedish crystalline rock.

The two SWIW-tests were carried out in a single fracture and a fracture zone, respectively. The single fracture at a depth of 422 m with a hydraulic transmissivity of $T = 1.0 \times 10^{-6} \text{ m}^2/\text{s}$ and the fracture zone at a depth of 576 m with a hydraulic transmissivity of $T = 5.2 \times 10^{-7} \text{ m}^2/\text{s}$. The model evaluation was made using a radial flow model with advection, dispersion and linear equilibrium sorption as transport processes.

A significant result from the SWIW-tests is that there is a very clear effect of retardation/sorption of Cesium in both the single fracture and in the fracture zone. The estimated value of the retardation factor for Cesium, $R = 90$ indicates a strong sorption. The value of R agrees approximately with values from cross-hole tests, obtained using similar transport models. Estimated tracer recovery at the last sampling time in the single fracture at 422 m yields approximately 86.2% and 40.7% for Uranine and Cesium, respectively and in the fracture zone at 576 m the respectively values for Uranine and Cesium are 80.5 and 51.6%. The model simulations were carried out for five different values of porosity; 0.002, 0.005, 0.01, 0.02, 0.05, resulting in estimates of longitudinal dispersivity within 0.36–2.50 m.

Sammanfattning

Denna rapport beskriver genomförandet, utvärderingen samt tolkningen av *in-situ* grundvattenflödesmätningar och enhålsspår försök (SWIW-test) i Laxemar och Simpevarp, Oskarshamn. Syftet med aktiviteten var dels att bestämma grundvattenflödet i enskilda sprickor och sprickzoner som skär borrhålen KLX02 och KSH02 samt att bestämma transportegenskaper för radionuklider i två potentiella flödesvägar genom att utföra och utvärdera SWIW-test i en enskild spricka och i en sprickzon i borrhål KSH02. Utspädningssonden användes också för vattenprovtagning (klass 5) i en enskild spricka på 957 m djup.

Grundvattenflödesmätningar genomfördes i 4 enskilda sprickor och i 3 sprickzoner på djup från 176 till 957 m. Hydrauliska transmissiviteten var inom intervallet $1,3 \times 10^{-8}$ – $7,4 \times 10^{-6}$ m²/s. Resultaten från utspädningmätningarna i borrhålen KSH02 och KLX02 visar att grundvattenflödet varierar avsevärt i sprickor och sprickzoner under naturliga ostörda hydrauliska förhållanden, ändå är generella trenden att flödet och Darcy hastigheten minskar mot djupet. Beräknade grundvattenflöden låg inom intervallet 0,09–2,81 ml/min och Darcy hastigheter från $3,4 \times 10^{-9}$ till $1,0 \times 10^{-7}$ m/s ($2,9 \times 10^{-4}$ – $8,6 \times 10^{-3}$ m/d), vilket är inom det förväntade området baserat på erfarenheter från tidigare genomförda utspädningmätningar under naturliga gradientförhållanden på andra platser i svenskt kristallint berg.

De två SWIW-testerna genomfördes i en enskild spricka på 422 m djup med T-värde $1,0 \times 10^{-6}$ m²/s samt i en sprickzon på 576 m djup med $T = 5,2 \times 10^{-7}$ m²/s. Utvärderingen gjordes med en radiell flödesmodell med advektion, dispersion och linjär jämviktssorption som transport processer.

Ett signifikant resultat från SWIW-testerna är en väldigt tydlig effekt av fördröjning/sorption av Cesium, både i den enskilda sprickan och i sprickzonen. Det av modellen bestämda värdet på retardationsfaktorn för Cesium, $R = 90$ indikerar en stark sorption. Värdet på R överensstämmer relativt bra med värden från flerhålsspår försök, erhållna med motsvarande transportmodeller. Den beräknade återhämtningen av spårämnen i återpumpningsfasen var cirka 86,2 % och 40,7 % för Uranin och Cesium respektive i den enskilda sprickan på 422 m djup. I sprickzonen på 576 m var återhämtningen cirka 80,5 och 51,6 % för respektive Uranin och Cesium. Modellpassningar till mätdata gjordes för fem olika värden på porositet; 0,002, 0,005, 0,01, 0,02, 0,05, vilket resulterade i longitudinell dispersivitet inom 0,36–2,50 m.

Contents

1	Introduction	7
2	Objective and scope	11
3	Equipment	13
3.1	Borehole dilution probe	13
3.1.1	Measurement range and accuracy	14
3.2	SWIW-test equipment	15
3.2.1	Measurement range and accuracy	16
4	Execution	17
4.1	Preparations	17
4.2	Procedure	17
4.2.1	Groundwater flow measurement	17
4.2.2	SWIW tests	18
4.2.3	Water sampling	18
4.3	Data handling	20
4.4	Analyses and interpretation	20
4.4.1	The dilution method – general principles	20
4.4.2	The dilution method – evaluation and analysis	22
4.4.3	SWIW test – basic outline	22
4.4.4	SWIW test – evaluation and analysis	22
4.5	Nonconformities	24
5	Results	25
5.1	Dilution measurements	25
5.1.1	KLX02, section 250.8–253.8 m	27
5.1.2	KLX02, section 338.4–341.4 m	28
5.1.3	KSH02, section 176.0–177.0 m	30
5.1.4	KSH02, section 422.3–423.3 m	31
5.1.5	KSH02, section 576.8–579.8 m	33
5.1.6	KSH02, section 858.6–859.6 m	34
5.1.7	KSH02, section 957.2–958.2 m	36
5.1.8	Summary of dilution results	37
5.2	SWIW tests	40
5.2.1	Treatment of experimental data	40
5.2.2	Tracer recovery breakthrough in KSH02, 422.3–423.3 m	40
5.2.3	Model evaluation KSH02, 422.3–423.3 m	42
5.2.4	Tracer recovery breakthrough in KSH02, 576.8–579.8 m	43
5.2.5	Model evaluation KSH02, 576.8–579.8 m	46
6	Discussion and conclusions	49
7	References	51
	Appendix A Borehole data KLX02 and KSH02	53
	Appendix B Dilution measurement KLX02	55
	Appendix C Dilution measurement KSH02	61

1 Introduction

SKB is currently conducting a site investigation in Oskarshamn, according to general and site specific programmes /SKB, 2001a,b/. Two, among several methods for site characterisation are *in-situ* groundwater flow measurements and single well injection withdrawal tests (SWIW-tests).

This document reports the results gained by SWIW tracer tests in borehole KSH02 and groundwater flow measurements with the borehole dilution probe in boreholes KLX02 and KSH02. The work was conducted by Geosigma AB and carried out in September 2003 in borehole KLX02, according to activity plan AP PU 400-03-005, and between January and October 2004 in borehole KSH02, according to activity plan AP PS 400-03-073. In Table 1-1 controlling documents for performing this activity are listed. Both activity plans and method descriptions are SKB's internal controlling documents. Data and results were delivered to the SKB site characterization database SICADA.

The borehole KLX02 is situated at the Laxemar site near Oskarshamn, Figures 1-1 and 1-2. KLX02 is a sub-vertical core borehole with a slight inclination of -85.0° from the horizontal plane. The borehole is in total 1,700 m deep and cased down to 203 m. From 203 m down to 1,700 m the diameter is 76 mm.

The borehole KSH02 is situated at the Simpevarp site near Oskarshamn, Figures 1-1 and 1-3. It is a sub-vertical core borehole with a slight inclination of -85.7° from the horizontal plane. The borehole is in total 1,001 m deep and cased down to 80 m. From 80 m down to 1,001 m the diameter is 76 mm.

Detailed information about the boreholes KLX02 and KSH02 are listed in Appendix A (excerpt from the SKB database SICADA).

Table 1-1. Controlling documents for the performance of the activity.

Activity plan	Number	Version
Aktivitetsplan för SAT av Utspädningssond med SWIW-test utrustning i borrhål KLX02.	AP PU 400-03-005	1.0
Grundvattenflödesmätningar och SWIW-tester med Utspädningssond i borrhål KSH02.	AP PS-400-03-073	1.0
Method descriptions	Number	Version
Metodbeskrivning för grundvattenflödesmätning.	SKB MD 350.001	1.0
Instruktion för längdkalibrering vid undersökningar i kärnborrhål.	SKB MD 620.010	1.0
Instruktion för rengöring av borrhålsutrustning och viss markbaserad utrustning.	SKB MD 600.004	1.0

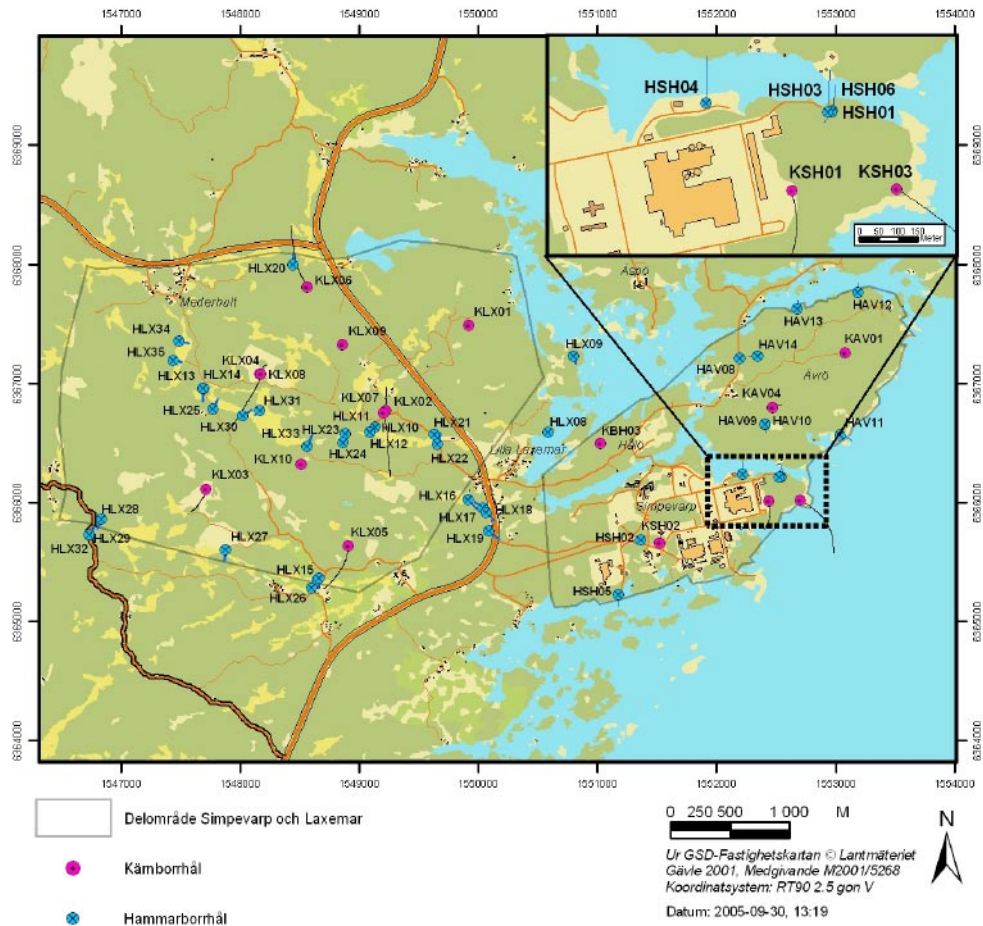


Figure 1-1. Overview of the Oskarshamn site investigation area, with sub areas Laxemar and Simpevarp, showing core boreholes (purple) and percussion boreholes (blue).

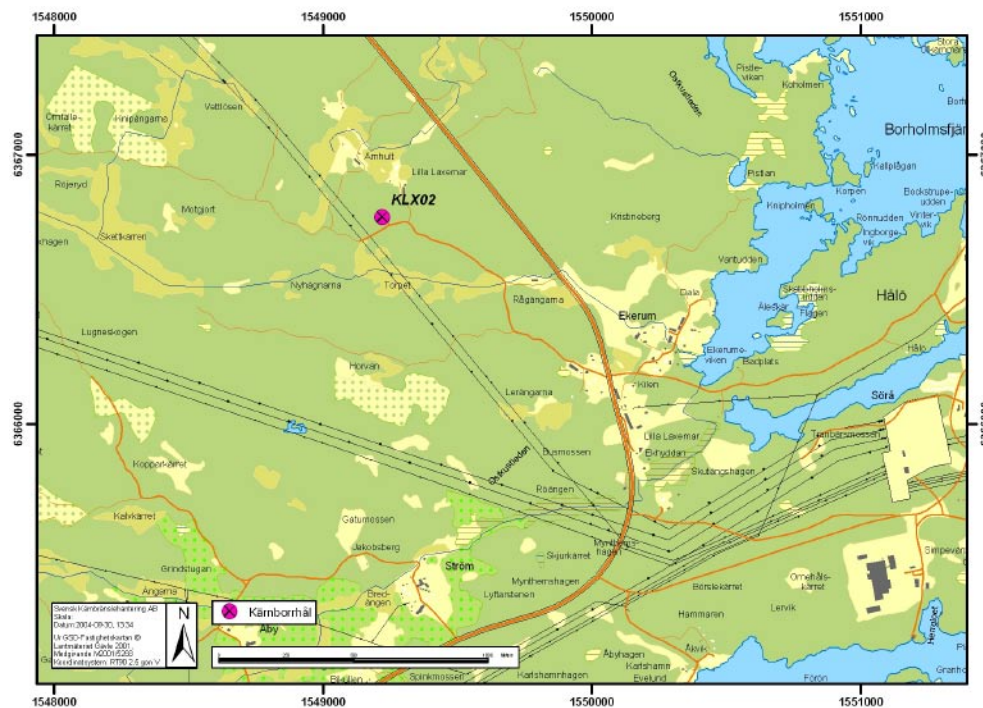


Figure 1-2. Location of borehole KLX02 in subarea Laxemar.

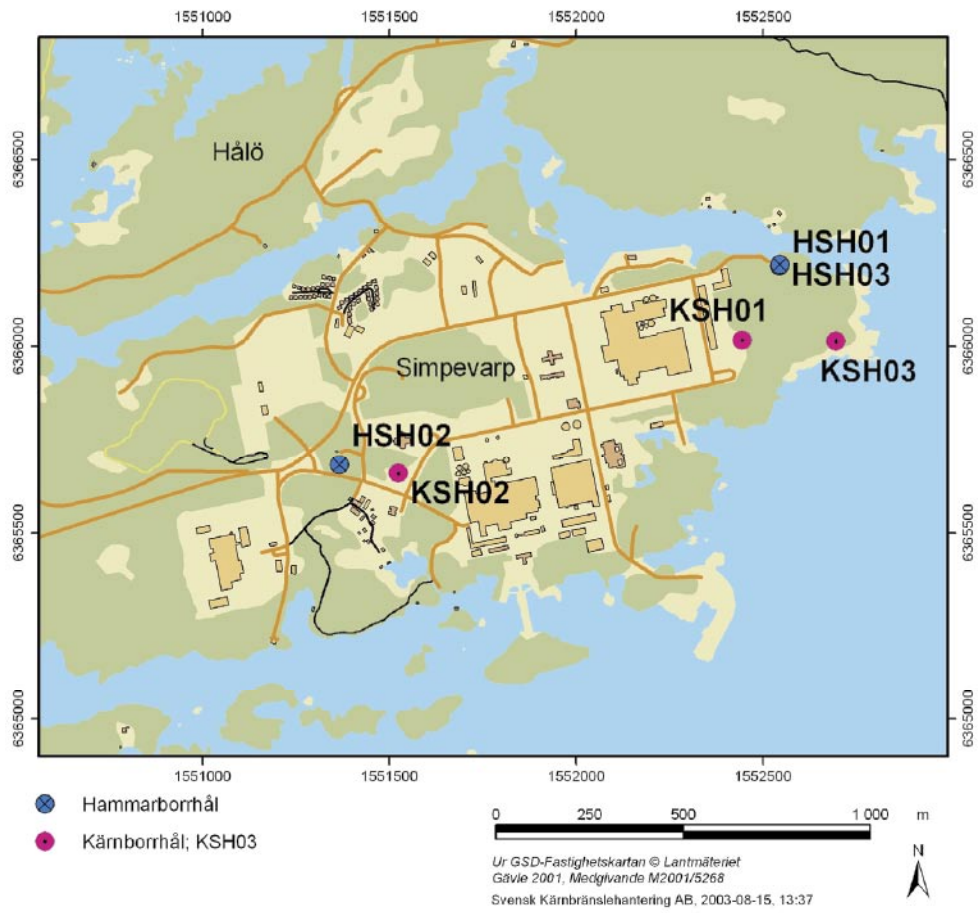


Figure 1-3. Location of borehole KSH02 in subarea Simpevarp.

2 Objective and scope

The objective of the activity was to measure ground water flow under a natural gradient in order to achieve information about natural flows and hydraulic gradients in the Simpevarp and Laxemar areas.

The objective of the SWIW tests was to determine transport properties of groundwater flow paths in fractures/fracture zones in a depth range of 300–700 m and a hydraulic transmissivity of 1×10^{-8} – 1×10^{-6} m²/s in the test section.

The groundwater flow measurements were performed in fractures and fracture zones at a depth range of 176–957 m using the SKB borehole dilution probe. The hydraulic transmissivity in the test sections ranged from 1.3×10^{-8} to 7.4×10^{-6} m²/s. Groundwater flow measurements were performed in totally seven test sections. In two of these sections SWIW tests were also performed, simultaneously using both a sorbing and a non-sorbing tracer.

The borehole dilution probe was also used to extract water samples for chemical characterisation of the waters in a fracture at 957 m depth in borehole KSH02.

3 Equipment

3.1 Borehole dilution probe

The borehole dilution probe is a mobile system for ground water flow measurements, Figure 3-1. Measurements can be made in boreholes with 56 mm or 76 mm diameter and the test section length can be arranged for 1, 2 or 3 m with an optimised special packer/dummy system and section length between 1 and 10 m with standard packers.

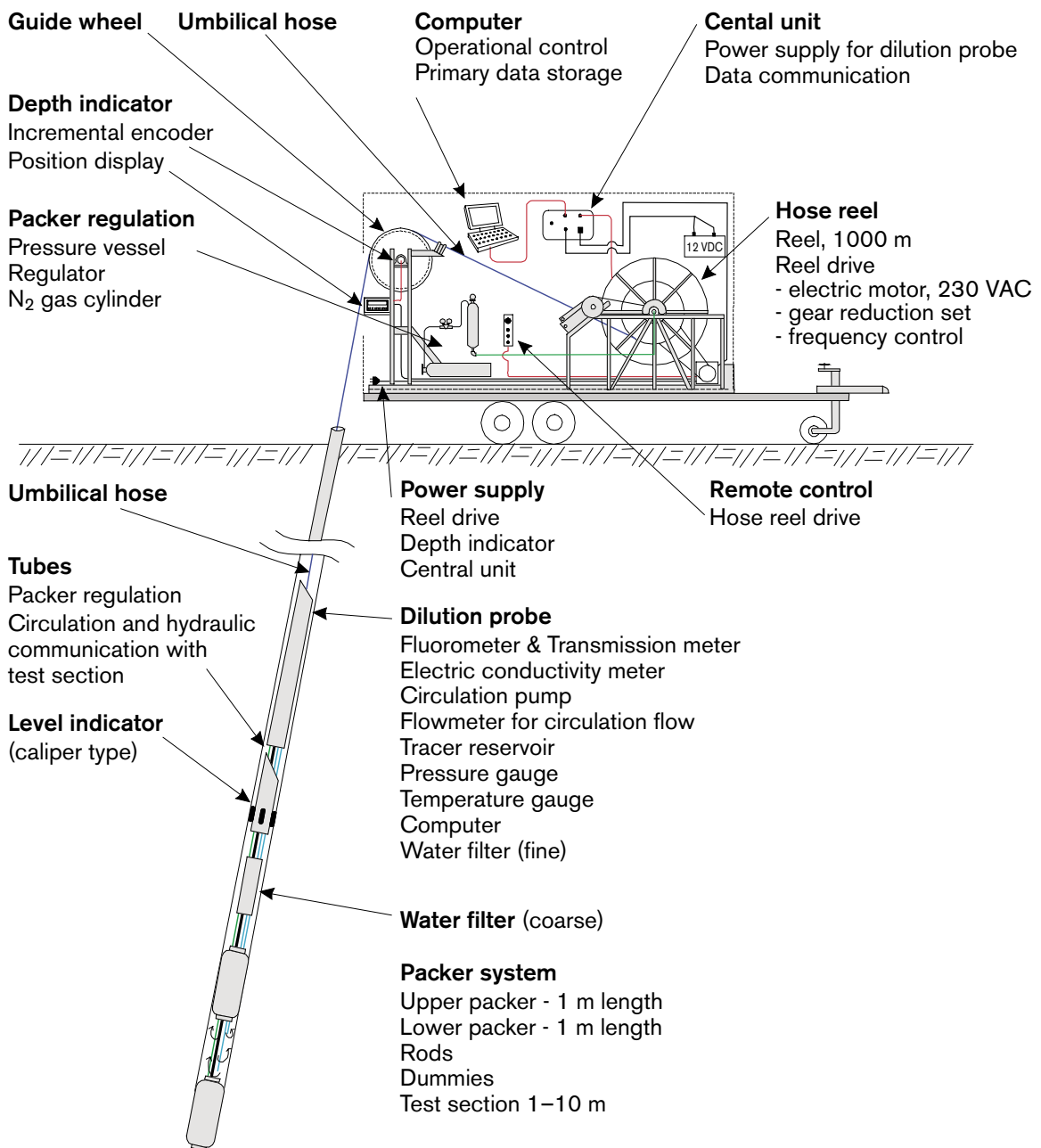


Figure 3-1. The SKB borehole dilution probe.

The maximum measurement depth is at 1,030 m borehole length. The main part of the equipment is the probe which measures the tracer concentration in the test section down hole and *in-situ*. The probe is equipped with two different measurement devices. One is the Optic device, which is a combined fluorometer and light-transmission meter. Several fluorescent and light absorbing tracers can be used with this device. The other device is the Electrical Conductivity device, which measures the electrical conductivity of the water and used for detection/analysis of saline tracers. The probe and the packers that straddle the test section are lowered in the borehole with an umbilical hose. The hose contains a tube for hydraulic inflation/deflation of the packers and electrical wires for power supply and communication/data transfer. Besides tracer dilution, the absolute pressure and temperature are also measured. The absolute pressure is measured during the process of dilution because a change in pressure indicates that the hydraulic gradient, and thus the groundwater flow, may have changed. The pressure gauge and the temperature gauge are both positioned in the dilution probe, about 7 metres from top of test section. This bias is not corrected for as only changes and trends relative to the start value are of great importance for the dilution measurement. Since the dilution method requires homogenous distribution of the tracer in the test section also a circulation pump is installed and circulation flow rate measured.

A caliper log, attached to the dilution probe, is used to position the probe and test section at the pre-selected borehole length. The caliper detects reference marks previously made by a drill bit at exact length along the borehole, approximately every 50 m. This method makes it possible to position the test section with an accuracy of $c \pm 0.10$ m.

3.1.1 Measurement range and accuracy

The lower limit of groundwater flow measurement is set by the dilution caused by molecular diffusion of the tracer into the fractured/porous aquifer, relative to the dilution of the tracer due to advective groundwater flow through the test section. In a normally fractured granite, the lower limit of a groundwater flow measurement is approximately at a hydraulic conductivity, K , between 6×10^{-9} and 4×10^{-8} m/s, if the hydraulic gradient, I , is 0.01. This corresponds to a groundwater flux (Darcy velocity), v , in the range of 6×10^{-11} to 4×10^{-10} m/s, which in turn may be transformed into groundwater flow rates, Q_w , corresponding to 0.03–0.2 ml/hour through a 1 m test section in a 76 mm diameter borehole. In a fracture zone with high porosity, and thus a higher rate of molecular diffusion from the test section into the fractures, the lower limit is about $K = 4 \times 10^{-7}$ m/s if $I = 0.01$. The corresponding flux value is in this case $v = 4 \times 10^{-9}$ m/s and flow rate $Q_w = 2.2$ ml/hour. The lower limit of flow measurements is, however, in most cases constrained by the time available for the dilution test. The required time frame for an accurate flow determination from a dilution test is within 7–60 hours at hydraulic conductivity values greater than about 1×10^{-7} m/s. At conductivity values below 1×10^{-8} m/s, measurement times should be at least 70 hours for natural undisturbed hydraulic gradient conditions.

The upper limit of groundwater flow measurements is determined by the capability of maintaining a homogeneous mix of tracer in the borehole test section. This limit is determined by several factors, such as length of the test section, volume, distribution of the water conducting fractures and how the circulation pump inlet and outlet are designed. The practical upper measurement limit is about 2,000 ml/hour for the equipment developed by SKB.

The accuracy of determined flow rates through the borehole test section is affected by various measurement errors related to, for example, the accuracy of the calculated test section volume and determination of tracer concentration. The overall accuracy when determining flow rates through the borehole test section is better than $\pm 30\%$, based on laboratory measurements in artificial borehole test sections.

The groundwater flow rates in the rock formation is determined from the calculated groundwater flow rates through the borehole test section and by using some assumption about the flow field around the borehole test section. This flow field depends on the hydraulic properties close to the borehole and is given by the correction factor α , as discussed in Chapter 4.4.2. The value of α will, at least, vary within $\alpha = 2 \pm 1.5$ in fractured rock /Gustafsson, 2002/. Hence, the groundwater flow in the rock formation is calculated with an accuracy of about $\pm 75\%$, depending on the flow-field distortion.

3.2 SWIW-test equipment

The SWIW (Single Well Injection Withdrawal) test equipment constitutes a complement to the borehole dilution probe making it possible to carry out a SWIW-test in the same test section as the dilution measurement, Figure 3-2. Measurements can be made in boreholes with 56 mm or 76 mm diameter and the test section length can be arranged for 1, 2 or 3 m with an optimised special packer/dummy system for 76 mm boreholes.

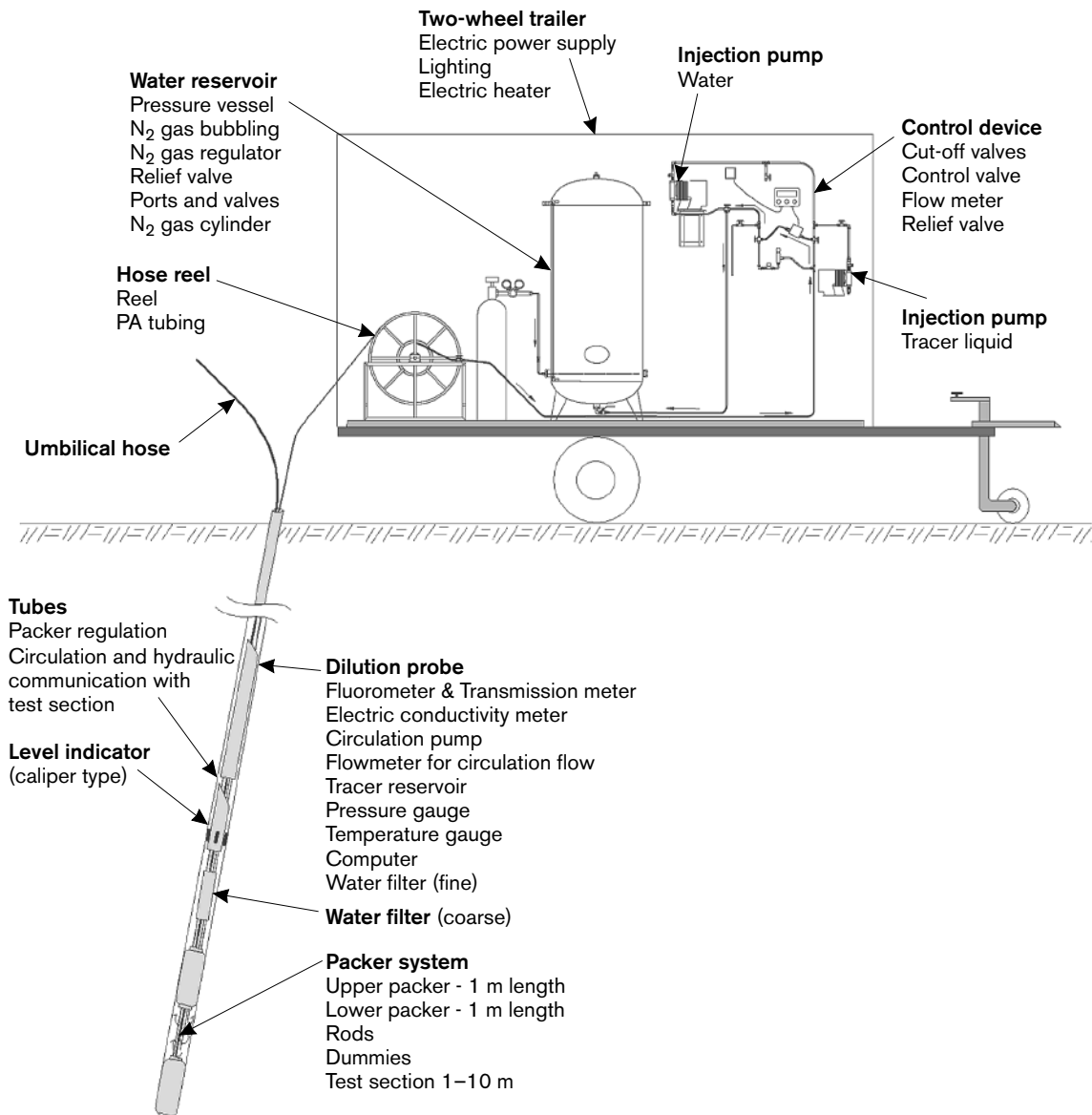


Figure 3-2. SWIW-test equipment, connected to the borehole dilution probe.

The equipment is designed for measurements in the depth interval 300–700 m borehole length. Besides the dilution probe the main parts of the SWIW-test equipment are:

- Polyamide tubing constituting the hydraulic connection between SWIW-test equipment at ground surface and the dilution probe in the borehole.
- Air tight vessel for storage of groundwater under anoxic conditions, i.e. N₂-atmosphere.
- Control system for injection of tracer solution and groundwater (chaser fluid).
- Injection pumps for tracer solution and groundwater.

3.2.1 Measurement range and accuracy

The result of a SWIW-test depends on the accuracy in the determination of the tracer concentration in injection solutions and withdrawn water. The result also depends on the accuracy in the determination of volume injection solution and volumes of injected and withdrawn water. For non-sorbing dye tracers (Uranine) the tracer concentration in collected water samples can be analysed with a resolution of 10 µg/l in the range 0.0–4.0 mg/l. The accuracy is within ± 5%. The volume of injected tracer solution can be determined within ± 0.1% and the volume of injected and withdrawn water determined within ± 5%.

The evaluation of a SWIW test and determination of transport parameters is done with model simulations, fitting the model to the measured data (concentration as a function of time). The accuracy in determined transport parameters depends on selection of model concept and how well the model fit the measured data.

4 Execution

The measurements were performed according to AP PU 400-03-005 and AP PS 400-03-073 (SKB internal controlling document) in accordance with the methodology descriptions for the borehole dilution probe equipment, – SKB MD 350.001 Metodbeskrivning för grundvattenflödesmätning-, and the measurement system description for SWIW-test, – SKB MD 353.069, MSB; Handhavande, SWIW-test utrustning- (SKB Internal controlling documents).

4.1 Preparations

Both the fluorometer and the electric conductivity meter were calibrated, according to SKB Internal controlling documents MD 353.015 and MD 353.017, before arriving at the site. Briefly, this was performed by adding certain amounts of the tracer to a known test volume while registering the measured A/D-levels. From this, calibration constants were calculated and saved for future use by using the measurement application. The other sensors had been calibrated previously (SKB MD 353.014 and 353.090) and were hence only control calibrated.

Extensive functionality checks were performed prior to transport to the site and limited function checks were performed at the site, according to SKB MD 353.065 and MD353.070.

The equipment was cleaned to comply with SKB cleaning level 1 (SKB MD 600.004) before lowering it into the borehole.

4.2 Procedure

4.2.1 Groundwater flow measurement

In total 7 groundwater flow measurements were performed, Table 4-1. Each measurement was performed according to the following procedure. The equipment was lowered to the right depth where background values of tracer concentration and supporting parameters, pressure and temperature, were measured and logged. Then, after inflating the packers and the pressure had stabilized, tracer was injected in the test section. The tracer concentration and supporting parameters were measured and logged continuously until the tracer had been diluted to such a degree that the groundwater flow rate could be calculated.

Table 4-1. Performed dilution measurements.

Borehole	Test section (m)	Number of flowing fractures*	T (m ² /s)*	Tracer	Dates (yymmdd–yymmdd)
KLX02	250.8–253.8	3	7.4E–6	NaCl	030918–030919
KLX02	338.4–341.4	3	6.0E–7	Uranine	030920–030921
KSH02	176.0–177.0	1	2.1E–7	Uranine	040204–040206
KSH02	422.3–423.3	1	1.0E–6	NaCl	040921–040923
KSH02	576.8–579.8	Fracture zone with 3–4 flowing fractures	5.2E–7	NaCl	041008–041011
KSH02	858.6–859.6	1	1.3E–8	Uranine	040219–040223
KSH02	957.2–958.2	1	5.4E–7	Uranine	040211–040216

* /Rouhiainen, 2000; Carlsten et al. 2001; Rouhiainen and Pöllänen, 2003/.

4.2.2 SWIW tests

Two SWIW tests were performed, Table 4-2. To conduct a SWIW test requires the SWIW equipment to be connected to the borehole dilution probe, Figures 4-1 and 4-2.

Table 4-2. Performed SWIW tests.

Borehole	Test section (m)	Number of flowing fractures*	T (m ² /s)*	Tracers	Dates (yymmdd–yymmdd)
KSH02	422.3–423.3	1	1.0E–6	Uranine / Cesium	040902–040921
KSH02	576.8–579.8	Fracture zone with 3–4 flowing fractures	5.2E–7	Uranine / Cesium	040929–041008

* /Rouhiainen, 2000, Carlsten et al. 2001, Rouhiainen and Pöllänen, 2003/.

The SWIW tests were performed according to the following procedure. The equipment was lowered to the right depth where background values of Uranine and supporting parameters, pressure and temperature, were measured and logged. Then, after inflating the packers and the pressure had stabilized, the circulation pump in the dilution probe was used to pump groundwater from the test section to the air tight vessel at the ground surface. Water samples were also taken for analysis of background concentration of Uranine and Cesium. When pressure had recovered after the pumping in the test section, the injection phases started with pre-injection of the native groundwater to reach steady state flow conditions. Thereafter injection of groundwater spiked with the tracers Uranine and Cesium and at last injection of native groundwater to push the tracers out into the fracture/fracture zone. After a short waiting phase, which was excluded in one test, the withdrawal phase started by pumping water to the ground surface. An automatic sampler at ground surface was used to take water samples for analysis of Uranine and Cesium in the withdrawn water.

4.2.3 Water sampling

The borehole dilution probe was also used for water sampling (class 5) in a single fracture at 958 m depth in borehole KSH02, contributing to the hydrochemical characterisation programme of the Simpevarp area, Table 4-3. The result of the chemical analysis is reported in /Wacker and Berg, 2004/.

Principle of flow determination

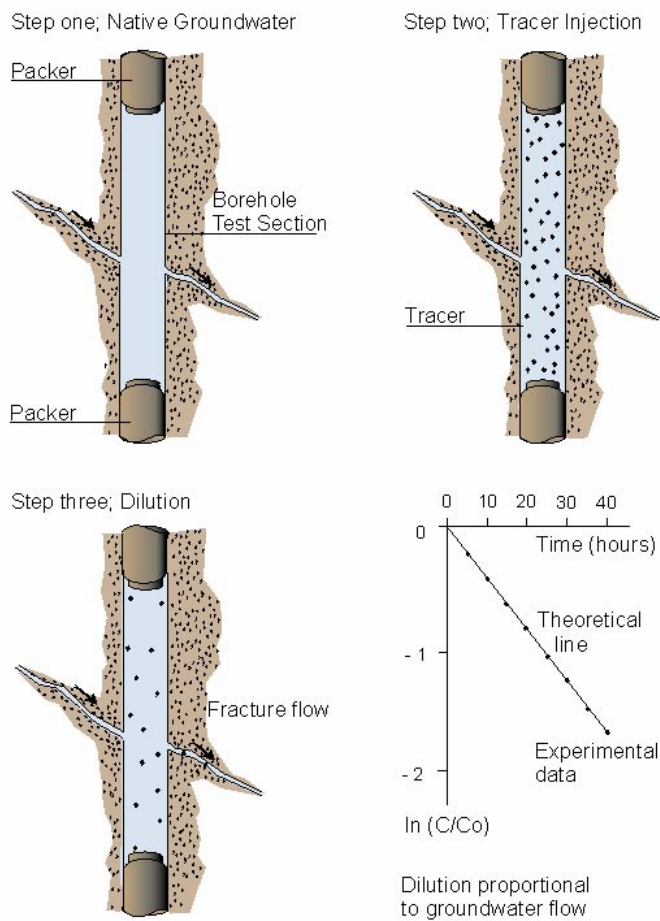


Figure 4-1. General principles of dilution and flow determination.

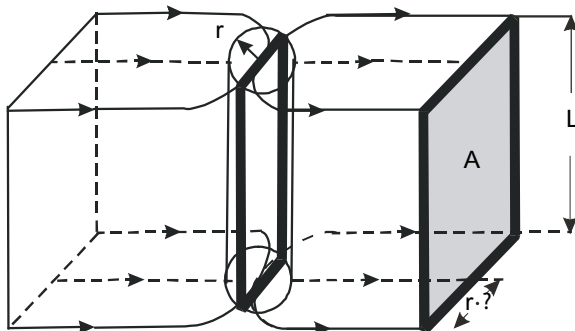


Figure 4-2. Diversion and conversion of flow lines in the vicinity of a borehole test section.

Table 4-3. Collected water samples.

Borehole	Section (m)	Dates (yymmdd–yymmdd)	Pumped volume (l)	Sampled volume (l)	Sample type	Sampling time
KSH02	957.2–958.2	040209–040211	720	30	Class 5	2004-02-11 10:40

4.3 Data handling

During a groundwater flow measurement with the dilution probe, data is automatically transferred from the measurement application to a Microsoft Access database. Data relevant for analysis and interpretation is then also automatically transferred from Access to Excel via an ODBC data link, set up by the operator. After each measurement the Excel data file is copied to a CD.

The water samples from the SWIW tests were analysed for Uranine tracer content at the Geosigma Laboratory in Uppsala and Cesium content was analysed at the Analytica laboratory in Luleå.

4.4 Analyses and interpretation

4.4.1 The dilution method – general principles

The dilution method is an excellent tool for *in-situ* determination of flow rates in fractures and fracture zones.

In the dilution method a tracer is introduced and homogeneously distributed into a bore-hole test section. The tracer is subsequently diluted by the ambient groundwater, flowing through the borehole test section. The dilution of the tracer is proportional to the water flow through the borehole section, Figure 4-1.

The dilution in a well-mixed borehole section, starting at time $t = 0$, is given by:

$$\ln(C / C_0) = -\frac{Q_w}{V} \cdot t \quad (\text{Equation 4-1})$$

where C is the concentration at time t (s), C_0 is the initial concentration, V is the water volume (m^3) in the test section and Q_w is the volumetric flow rate (m^3s^{-1}). Since V is known, the flow rate may then be determined from the slope of the line in a plot of $\ln(C/C_0)$, or $\ln C$, versus t .

An important interpretation issue is to relate the measured groundwater flow rate through the borehole test section to the rate of groundwater flow in the fracture/fracture zone straddled by the packers. The flow-field distortion must be taken into consideration, i.e. the degree to which the groundwater flow converges and diverges in the vicinity of the borehole test section. With a correction factor, α , which accounts for the distortion of the flow lines due to the presence of the borehole, it is possible to determine the cross-sectional area perpendicular to groundwater flow by:

$$A = 2 \cdot r \cdot L \cdot \alpha \quad (\text{Equation 4-2})$$

where A is the cross-sectional area (m^2) perpendicular to groundwater flow, r is borehole radius (m), L is the length (m) of the borehole test section and α is the correction factor. Figure 4-2 schematically shows the cross-sectional area, A , and how flow lines converge and diverge in the vicinity of the borehole test section.

Assuming laminar flow in a plane parallel fissure or a homogeneous porous medium, the correction factor α is calculated according to Equation (4-3), which often is called the formula of Ogilvi /Halevy et al. 1967/. Here it is assumed that the disturbed zone, created by the presence of the borehole, has an axis-symmetrical and circular form.

$$\alpha = \frac{4}{1 + (r/r_d) + (K_2/K_1)(1 - (r/r_d)^2)} \quad \text{(Equation 4-3)}$$

where r_d is the outer radius (m) of the disturbed zone, K_1 is the hydraulic conductivity (m/s) of the disturbed zone, and K_2 is the hydraulic conductivity of the aquifer. If the drilling has not caused any disturbances outside the borehole radius, then $K_1 = K_2$ and $r_d = r$ which will result in $\alpha = 2$. With $\alpha = 2$, the groundwater flow within twice the borehole radius will converge through the borehole test section, as illustrated in Figures 4-2 and 4-3.

If there is a disturbed zone around the borehole the correction factor α is given by the radial extent and hydraulic conductivity of the disturbed zone. If the drilling has caused a zone with a lower hydraulic conductivity in the vicinity of the borehole than in the fracture zone, e.g. positive skin due to drilling debris and clogging, the correction factor α will decrease. A zone of higher hydraulic conductivity around the borehole will increase α . Rock stress redistribution, when new boundary conditions are created by the drilling of the borehole, may also change the hydraulic conductivity around the borehole and thus affect α . In Figure 4-3, the correction factor, α , is given as a function of K_2/K_1 at different normalized radial extents of the disturbed zone (r/r_d). If the fracture/fracture zone and groundwater flow is not perpendicular to the borehole axis, this also has to be accounted for. At a 45 degree angle to the borehole axis the value of α will be about 41% larger than in the case of perpendicular flow. This is further discussed in /Gustafsson, 2002/ and /Rhén et al. 1991/.

In order to obtain the Darcy velocity in the undisturbed rock the calculated ground water flow, Q_w is divided by A, Equation 4-4.

$$v = Q_w / A \quad \text{(Equation 4-4)}$$

The hydraulic gradient is then calculated as

$$I = v/K \quad \text{(Equation 4-5)}$$

where K is the hydraulic conductivity.

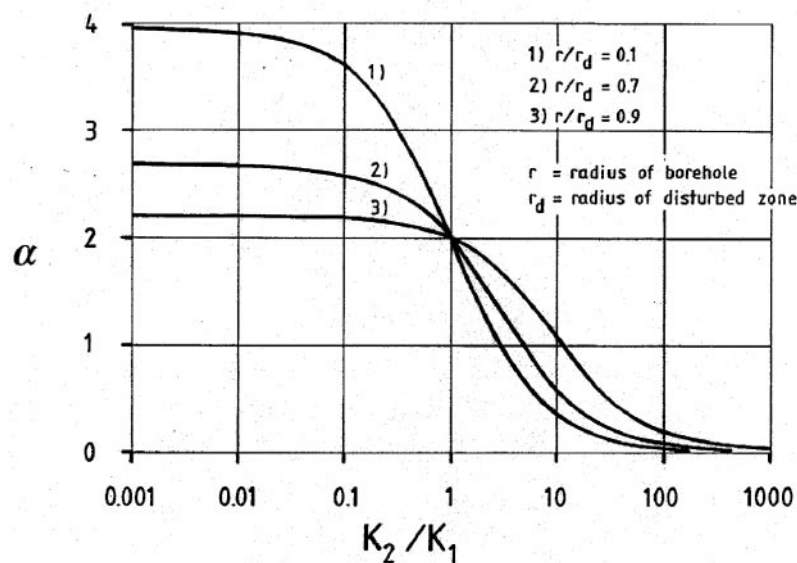


Figure 4-3. The correction factor, α , as a function of K_2/K_1 at different radial extent (r/r_d) of the disturbed zone (skin zone) around the borehole.

4.4.2 The dilution method – evaluation and analysis

The first step of evaluation included studying a graph of the measured concentration versus time data. For further evaluation background concentration, i.e. any tracer concentration in the groundwater before tracer injection, was subtracted from the measured concentrations. Thereafter $\ln(C/C_0)$ was plotted versus time. In most cases that relationship was linear and the proportionality constant was then calculated by performing a linear regression. In the cases where the relationship between $\ln(C/C_0)$ and time was non-linear, a sub-interval was chosen in which the relationship were linear.

The value of $\ln(C/C_0)/t$ obtained from the linear regression was then used to calculate Q_w according to Equation (4-1).

The hydraulic gradient, I , was calculated by combining Equations (4-2), (4-4) and (4-5), and choosing $\alpha = 2$. The hydraulic conductivity, K , in Equation (4-5) was obtained from previously performed Difference flow measurements /Rouhiainen, 2000; Carlsten et al. 2001; Rouhiainen and Pöllänen, 2003/.

4.4.3 SWIW test – basic outline

A Single Well Injection Withdrawal (SWIW) test may consist of all or some of the following phases:

1. filling-up pressure vessel with groundwater from the selected fracture,
2. injection of water to establish steady state hydraulic conditions (pre-injection),
3. injection of one or more tracers,
4. injection of groundwater (chaser fluid) after tracer injection is stopped,
5. waiting phase,
6. withdrawal (recovery) phase.

The tracer breakthrough data that is eventually used for evaluation is obtained from the withdrawal phase. The injection of chaser fluid, i.e. groundwater from the pressure vessel, has the effect of pushing the tracer out as a “ring” in the formation surrounding the tested section. This is generally a benefit because when the tracer is pumped back both ascending and descending parts are obtained in the recovery breakthrough curve. During the waiting phase there is no injection or withdrawal of fluid. The purpose of this phase is to increase the time available for time-dependent transport-processes so that these may be more easily evaluated from the resulting breakthrough curve. A schematic example of a resulting breakthrough curve during a SWIW test is shown in Figure 4-4.

The design of a successful SWIW test requires prior determination of injection and withdrawal flow rates, duration of tracer injection, duration of the various injection, waiting and pumping phases, selection of tracers, tracer injection concentrations, etc.

4.4.4 SWIW test – evaluation and analysis

The model evaluation of the experimental results was carried out assuming homogenous conditions. Model simulations were made using the model code SUTRA /Voss, 1984/ and the experiments were simulated without a background hydraulic gradient. It was assumed that flow and transport occurs within a planar fracture zone of some thickness. The volume available for flow was represented by assigning a porosity value to the assumed zone. Modelled transport processes include advection, dispersion and linear equilibrium sorption.

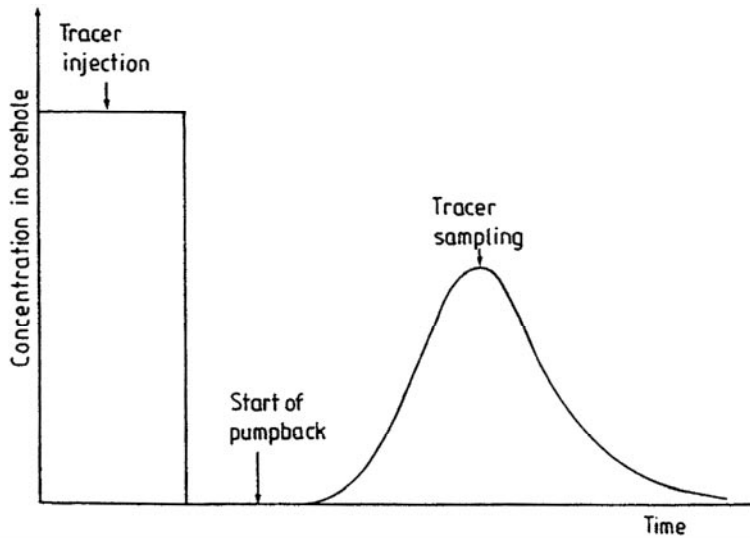


Figure 4-4. Schematic tracer concentration sequence during a SWIW test /Andersson, 1995/.

The sequence of the different injection phases were modelled as accurately as possible based on supporting data for flows and tracer injection concentration. Generally, experimental flows and times may vary from one phase to another, and the flow may also vary within phases. The specific experimental sequences for the borehole sections are listed in the sections below.

In the simulation model, tracer injection was simulated as a function accounting for mixing in the borehole section and sorption (for Cesium) on the borehole walls. The function assumes a completely mixed borehole section and linear equilibrium surface sorption:

$$C = (C_0 - C_{in})e^{-\left(\frac{Q}{V_{bh} + K_a A_{bh}}\right)t} + C_{in} \quad \text{(Equation 4-6)}$$

where C is concentration in water leaving the borehole section, and entering the formation (kg/m^3), V_{bh} is the borehole volume including circulation tubes (m^3), A_{bh} is area of borehole walls (m^2), Q is flow rate (m^3/s), C_{in} is concentration in the water entering the borehole section (kg/m^3), C_0 is initial concentration in the borehole section (kg/m^3), K_a is surface sorption coefficient (m) and t is elapsed time (s).

The sorption coefficient K_a was assigned a value of 10^{-2} m in all simulations. An example of the tracer injection input function is given in Figure 4-5, showing a 50 minutes long tracer injection phase followed by a chaser phase.

Non-linear regression was used to fit the simulation model to experimental data. The estimation strategy was generally to estimate the dispersivity (a_L) and a retardation factor (R), while setting the porosity (i.e. the available volume for flow) to a fixed value. Simultaneous fitting of both tracer breakthrough curves (Uranine and Cesium), and calculation of fitting statistics, was carried out using the approach described in /Nordqvist and Gustafsson, 2004/.

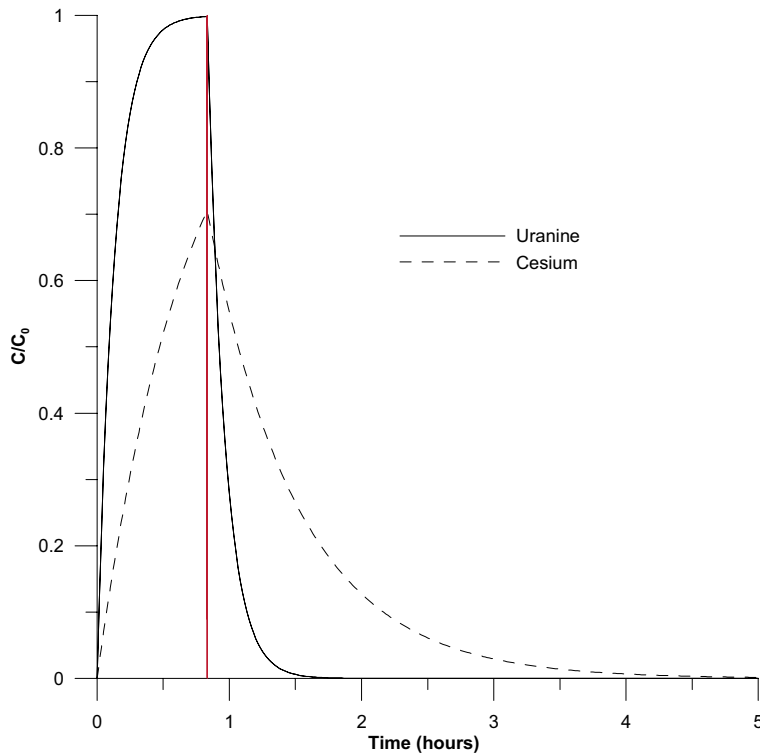


Figure 4-5. Example of simulated tracer injection functions for a tracer injection (ending at 50 minutes shown by the vertical red line) phase immediately followed by a chaser phase.

4.5 Nonconformities

All test sections proposed in AP PS-400-03-073 for groundwater flow measurements in borehole KSH02 could not be measured due to technical problems with the equipment (packers and probe), borehole water (dirty) and borehole casing (equipment got stuck). The SWIW test in section 422.3–423.3 m was prolonged with a second chaser fluid injection and waiting phase due to borehole probe and packer system had to be hoisted to the ground surface for repair after the first waiting phase, se Chapter 5.2.2 and Table 5-2.

5 Results

The primary data and original results are stored in the SKB database SICADA. These data shall be used for further interpretation or modelling.

5.1 Dilution measurements

Figure 5-1 exemplifies a typical dilution curve in a single fracture straddled by the test section at 858.6–859.6 m depth in borehole KSH02. In the first phase the background value is recorded for about five hours. In phase two Uranine tracer is injected and after mixing, a start concentration (C_0) of about 4.5 mg/l is achieved. In phase three the dilution is measured for about 95 hours. Thereafter the packers are deflated and the remaining tracer flows out of the test section. Figure 5-2 shows the measured pressure during the dilution measurement. Since the pressure gauge is positioned about 7 metres from top of test section there is a bias from the pressure in the test section which is not corrected for, as only changes and trends relative to the start value are of great importance for the dilution measurement. In this case diurnal pressure variations due to earth tidal effects are visible. Otherwise the natural pressure is in a slowly decreasing trend. Figure 5-3 is a plot of the $\ln(C/C_0)$ versus time data and linear regression best fit to data showing a good fit with correlation $R^2 = 0.9971$. Calculated groundwater flow rate, Darcy velocity and hydraulic gradient is presented in Table 5-1 together with the results from all other dilution measurements carried out in boreholes KLX02 and KSH02.

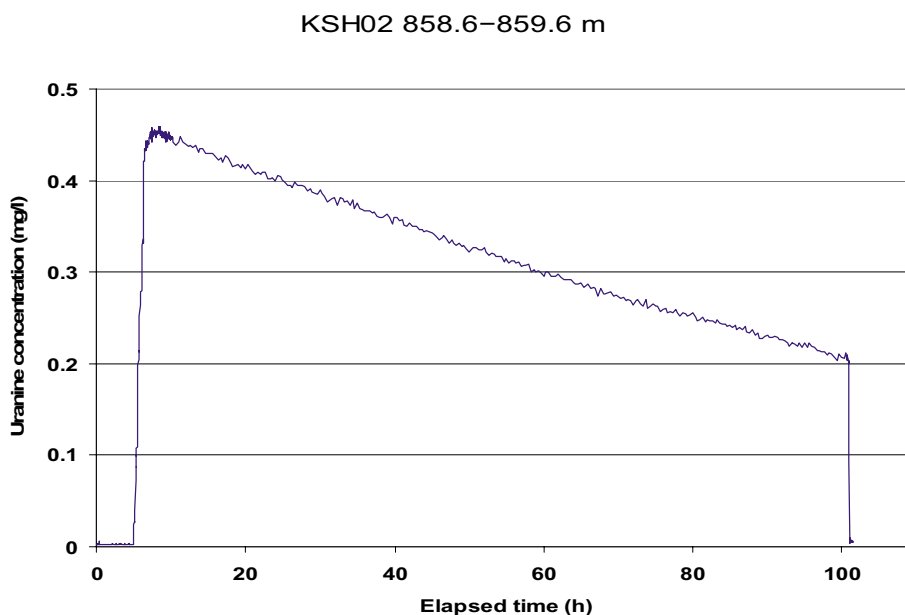


Figure 5-1. Dilution measurement in borehole KSH02, section 858.6–859.6 m.

KSH02 858.6–859.6 m

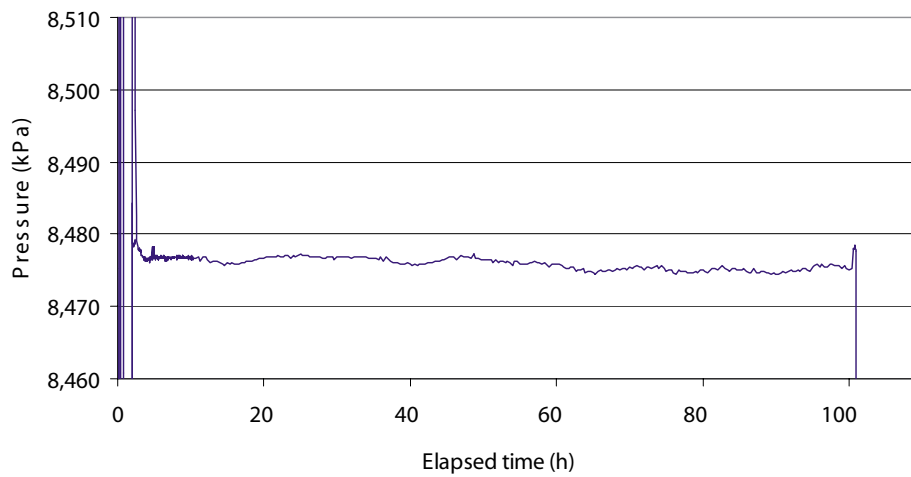


Figure 5-2. Measured pressure during dilution measurement in borehole KSH02, section 858.6–859.6 m.

KSH02 858.6–859.6 m

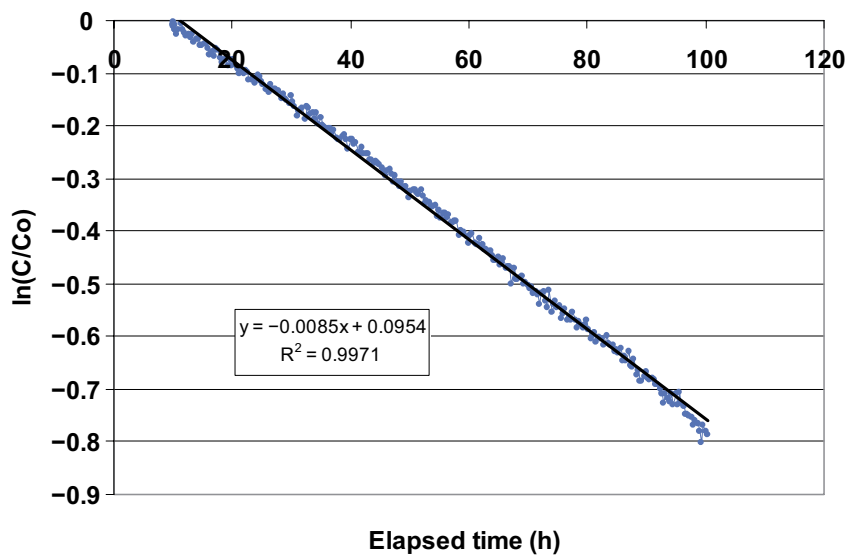


Figure 5-3. Linear regression best fit to data from dilution measurement in borehole KSH02, section 858.6–859.6 m.

The dilution measurements were carried out either with the dye tracer Uranine or the saline tracer NaCl. In borehole KSH02 Uranine tracer was the first choice because it normally has a low background concentration and the tracer can be injected and measured in concentrations far above the background value, which gives a large dynamic range and accurate flow determinations. However, in some test sections precipitations and groundwater composition made it impossible to perform *in-situ* measurements of Uranine with the fluorescence technique. NaCl tracer, measured by means of electric conductivity, was then used instead. The drawback with NaCl measurements is the high background concentration at larger depth. Changes in the background concentration will have a considerable impact on the measured tracer concentration in the test section, and thus also on the determined groundwater flow rate. In borehole KLX02 the dilution measurements constituted a part of a site acceptance test where the tracer selections were decided in advance.

Details of all dilution measurements, with diagrams of dilution versus time and the supporting parameters pressure, temperature and circulation flow rate are presented in Appendix B1–B2 and C1–C5.

5.1.1 KLX02, section 250.8–253.8 m

This dilution measurement was carried out with the saline tracer NaCl in a test section with three flowing fractures. The complete test procedure can be followed in Figure 5-4. Background concentration (0.18 g/l) is measured for about four hours. Thereafter the NaCl tracer is injected in four steps and after mixing it finally reaches a start concentration of 2.83 g/l above background. Dilution is measured for about 11 hours, the packers are then deflated and the remaining tracer flows out of the test section. The concentration versus time seems to follow a perfect dilution according to theory, but the complete set of the $\ln(C/C_0)$ versus time data could not fit a straight line ($R^2 = 0.955$). Hydraulic pressure shows no major variations but a very slow decreasing trend is visible for the first 13 hours of elapsed time (Appendix B1). For these two reasons the final evaluation was made on the last part of the dilution measurement, from 13 to 17 hours of elapsed time. The correlation coefficient of the best fit line is $R^2 = 0.970$ (Figure 5-5), and the groundwater flow rate, calculated from the best fit line, is 2.81 ml/min. Calculated hydraulic gradient is 0.042 and Darcy velocity 1.03×10^{-7} m/s.

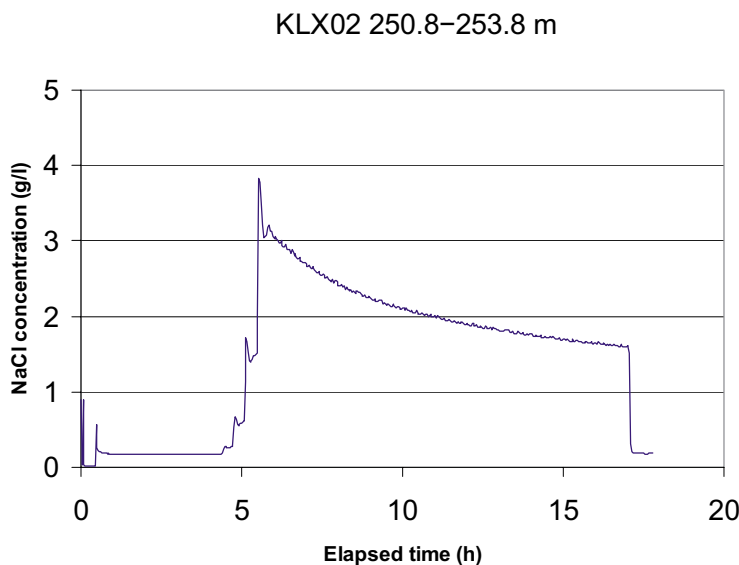


Figure 5-4. Dilution measurement in borehole KLX02, section 250.8–253.8 m.

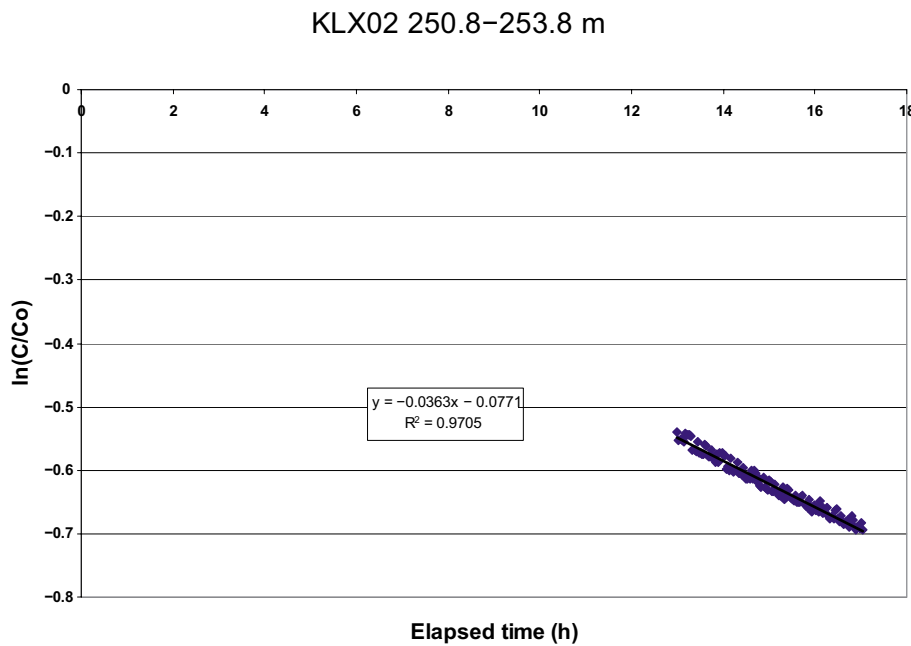


Figure 5-5. Linear regression best fit to data from dilution measurement in borehole KLX02, section 250.8–253.8 m.

5.1.2 KLX02, section 338.4–341.4 m

This dilution measurement was carried out with the dye tracer Uranine in a test section with three flowing fractures. The background measurement, tracer injection and dilution can be followed in Figure 5-6. Background concentration is close to zero. The Uranine tracer is injected in two steps and after mixing it reaches a start concentration of 0.90 mg/l above background. Dilution is measured for about 15 hours. Thereafter the packers are deflated, but this and succeeding activities of the dilution measurement were not logged in this case. Hydraulic pressure shows a slow decreasing trend during the dilution measurement, i.e. 7–22 hours of elapsed time (Appendix B2). A linear relationship between $\ln(C/C_0)$ and time could not be improved by choosing a sub-interval of the dilution measurement. The complete set of $\ln(C/C_0)$ versus time data was therefore used for determination of groundwater flow. The regression line fits well to the slope of the dilution but the scattered measurement data results in a correlation coefficient of $R^2 = 0.895$ for the best fit line (Figure 5-7). The groundwater flow rate, calculated from the best fit line, is 0.42 ml/min. Calculated hydraulic gradient is 0.077 and Darcy velocity 1.54×10^{-8} m/s. The hydraulic gradient is judged as large, but nothing in the dilution measurement or the measured supporting parameters can be found that contradicts the calculated gradient.

KLX02 338.4–341.4 m

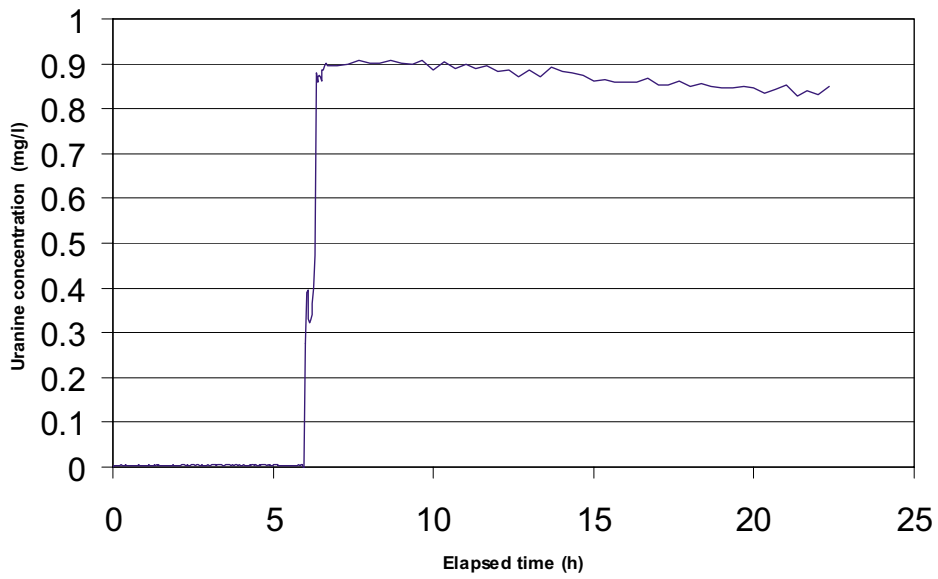


Figure 5-6. Dilution measurement in borehole KLX02, section 338.4–341.4 m.

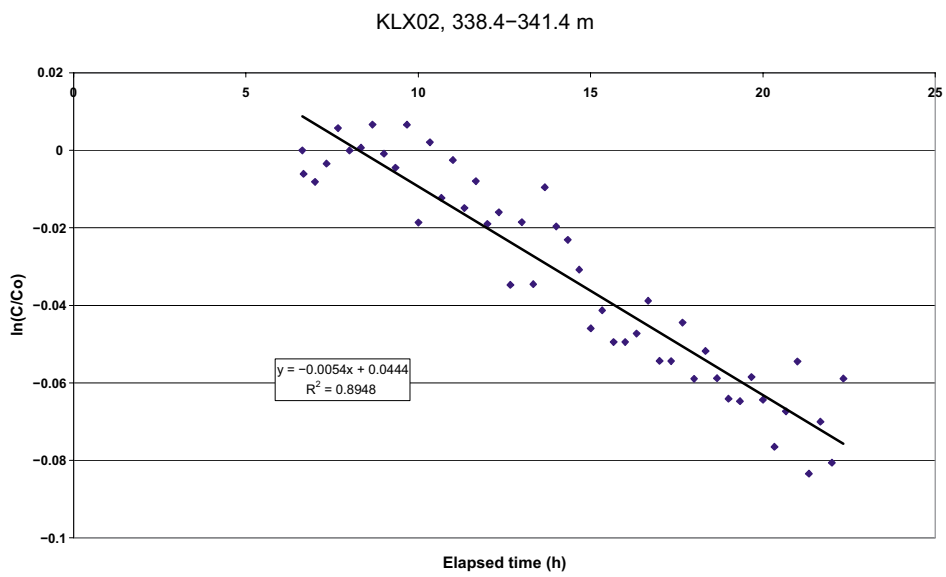


Figure 5-7. Linear regression best fit to data from dilution measurement in borehole KLX02, section 338.4–341.4 m.

5.1.3 KSH02, section 176.0–177.0 m

This dilution measurement was carried out in a single fracture with the dye tracer Uranine. The background measurement, tracer injection and dilution can be followed in Figure 5-8. Background concentration is close to zero. The Uranine tracer is injected in two steps and after mixing it reaches a start concentration of 0.33 mg/l above background. Dilution is measured for about 37 hours. Thereafter the packers are deflated, but this and succeeding activities of the dilution measurement were not logged in this case. Hydraulic pressure indicates a very small increasing trend. Small diurnal pressure variations due to earth tidal effects are also visible (Appendix C1). The complete set of $\ln(C/C_0)$ versus time data was used for determination of groundwater flow. The regression line fits well to the slope of the dilution with a correlation coefficient of $R^2 = 0.993$ for the best fit line (Figure 5-9). The groundwater flow rate, calculated from the best fit line, is 0.65 ml/min. Calculated hydraulic gradient is 0.347 and Darcy velocity 7.18×10^{-8} m/s. The hydraulic gradient is very large. It is not clear if the large gradient is caused by local effects where the measured fracture constitutes a hydraulic conductor between other fractures with different hydraulic heads or due to wrong estimates of the correction factor, α , and/or the hydraulic conductivity of the fracture. However, hydraulic gradients, calculated according to the Darcy concept, are also large in the single fractures at 858.6 and 957.2 m borehole length.

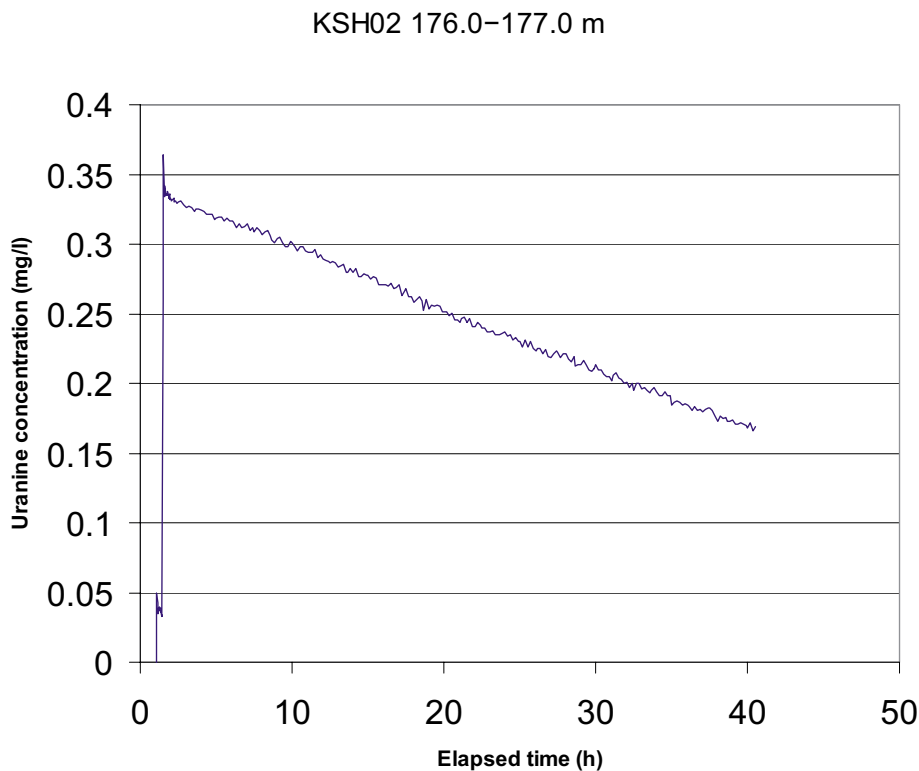


Figure 5-8. Dilution measurement in borehole KSH02, section 176.0–177.0 m.

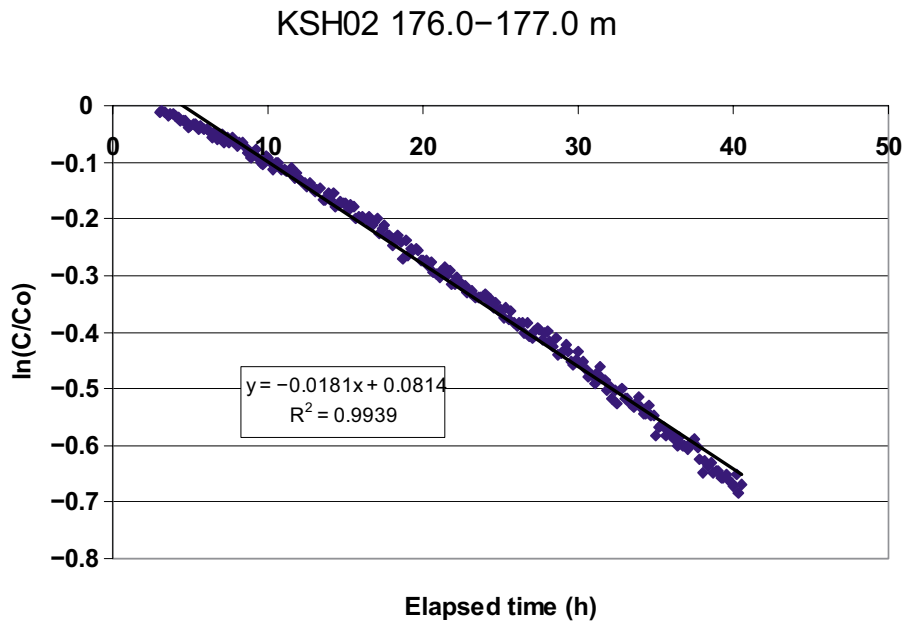


Figure 5-9. Linear regression best fit to data from dilution measurement in borehole KSH02, section 176.0–177.0 m.

5.1.4 KSH02, section 422.3–423.3 m

This dilution measurement was carried out in a single fracture with the saline tracer NaCl. The background measurement, tracer injection and dilution can be followed in Figure 5-10. Background concentration (13.0 g/l) is measured for about one hour. Thereafter the NaCl tracer is injected in four steps and after mixing it finally reaches a start concentration of 30 g/l, i.e. 17 g/l above background. Dilution is measured for about 45 hours. Thereafter the packers are deflated, but this and succeeding activities of the dilution measurement were not logged in this case. The data shows scattered peaks, especially during the first 30 hours of elapsed time. They are believed artefacts due to some electronic disturbances caused by e.g. earth currents. After about 40 hours of elapsed time there is a sudden drop in measured concentrations, which can't be explained and therefore this part of the dilution is excluded in the further evaluation. Hydraulic pressure indicates a very small increasing trend. A diurnal pressure variation due to earth tidal effects is also visible (Appendix C2). Groundwater flow is determined from the 6–40 hours part of the dilution measurement. The regression line shows an acceptable fit to the $\ln(C/C_0)$ versus time data with a correlation coefficient of $R^2 = 0.859$ for the best fit line (Figure 5-11). The groundwater flow rate, calculated from the best fit line, is 0.19 ml/min. Calculated hydraulic gradient is 0.021 and Darcy velocity 2.15×10^{-8} m/s.

KSH02 422.3–423.3 m

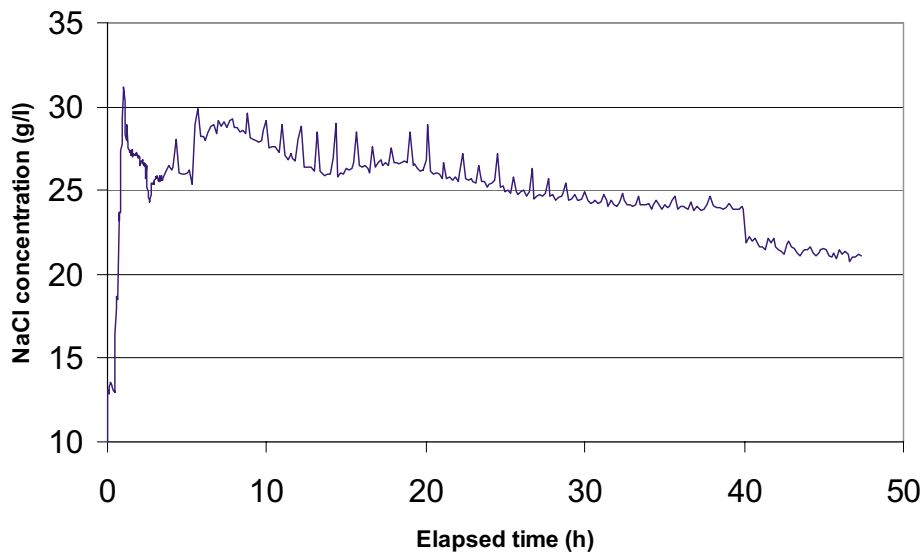


Figure 5-10. Dilution measurement in borehole KSH02, section 422.3–423.3 m.

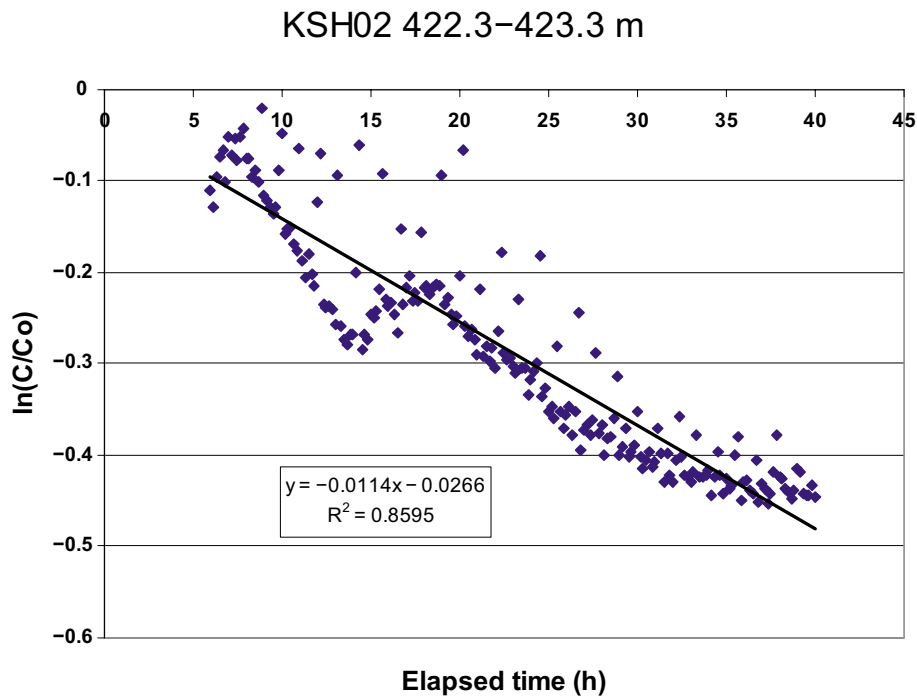


Figure 5-11. Linear regression best fit to data from dilution measurement in borehole KSH02, section 422.3–423.3 m.

5.1.5 KSH02, section 576.8–579.8 m

This dilution measurement was carried out with the saline tracer NaCl in a fracture zone with 3–4 flowing fractures. The concentration versus time data is presented in Figure 5-12, but it is difficult to follow the test procedure because of the scattered data in the beginning and at the end of the test. Background concentration is determined at 13.4 g/l and the start concentration 16 g/l, i.e. only 2.6 g/l above background. Dilution is measured for about 60 hours. Thereafter the packers are deflated at 72 hours of elapsed time. Hydraulic pressure increases slowly during the first 50 hours of elapsed time and thereafter it is more or less stable (Appendix C3). Groundwater flow is determined from the 20–60 hours part of the dilution measurement. The regression line shows an acceptable fit to the $\ln(C/C_0)$ versus time data but the scattered measurement data results in a correlation coefficient of $R^2 = 0.281$ for the best fit line (Figure 5-13). The groundwater flow rate, calculated from the best fit line, is 0.09 ml/min. Calculated hydraulic gradient is 0.020 and Darcy velocity 3.44×10^{-9} m/s.

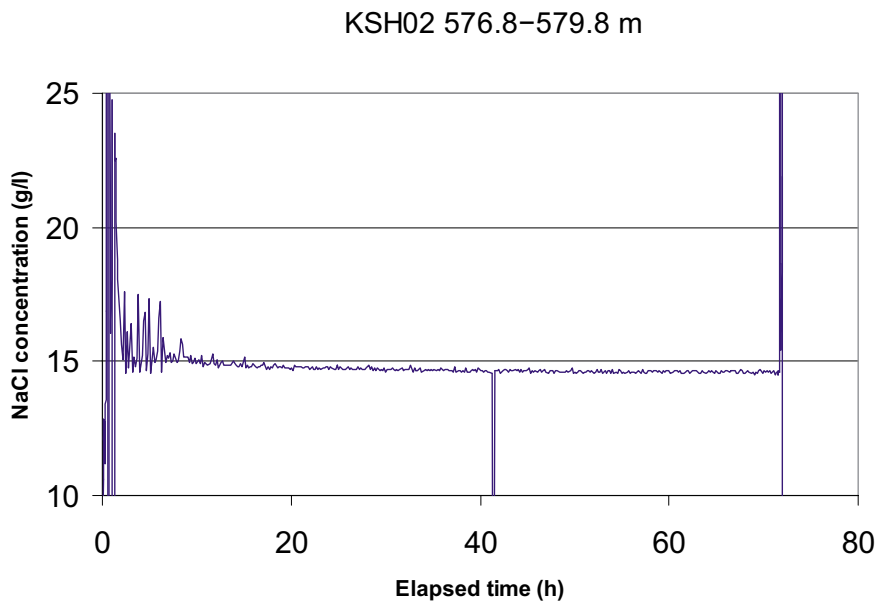


Figure 5-12. Dilution measurement in borehole KSH02, section 576.8–579.8 m.

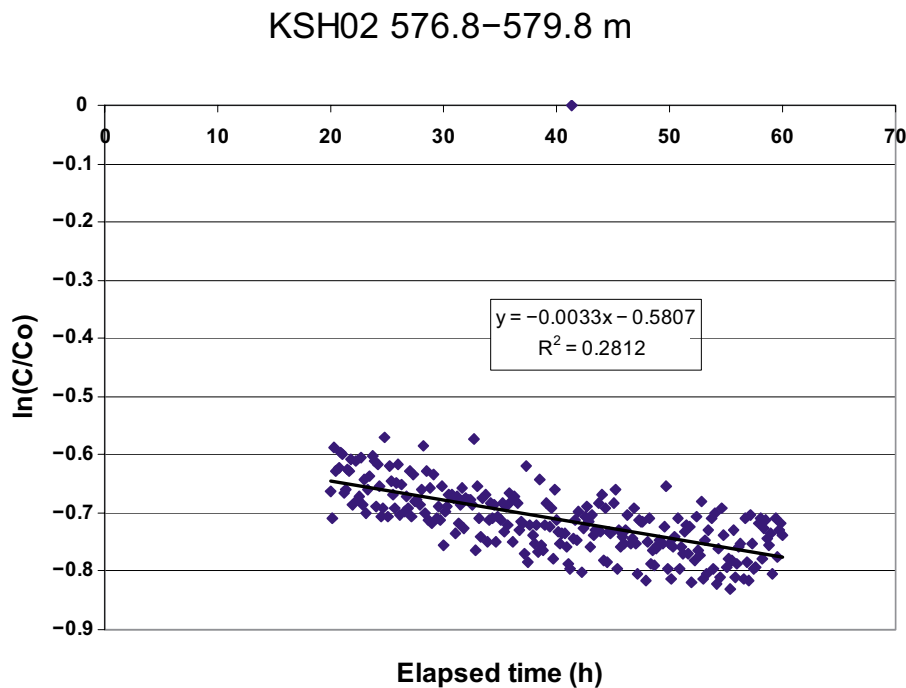


Figure 5-13. Linear regression best fit to data from dilution measurement in borehole KSH02, section 576.8–579.8 m.

5.1.6 KSH02, section 858.6–859.6 m

This dilution measurement was carried out in a single fracture with the dye tracer Uranine. The background measurement, tracer injection and dilution can be followed in Figure 5-14. Background concentration is close to zero. The Uranine tracer is injected in six steps and after mixing it reaches a start concentration of 0.45 mg/l above background. Dilution is measured for about 90 hours. Thereafter the packers are deflated and the remaining tracer flows out of the test section. Hydraulic pressure indicates a very small decreasing trend. Small diurnal pressure variations due to earth tidal effects are also visible (Appendix C4). The complete set of $\ln(C/C_0)$ versus time data, i.e. 10–100 hours of elapsed time, was used for determination of groundwater flow. The regression line fits well to the slope of the dilution with a correlation coefficient of $R^2 = 0.997$ for the best fit line (Figure 5-15). The groundwater flow rate, calculated from the best fit line, is 0.31 ml/min. Calculated hydraulic gradient is 2.570 and Darcy velocity is 3.41×10^{-8} m/s. The hydraulic gradient is very large and may be caused by a hydraulic shortcut or wrong estimates of correction factor, α , and/or the hydraulic conductivity as discussed in Chapter 5.1.3.

KSH02 858.6–859.6 m

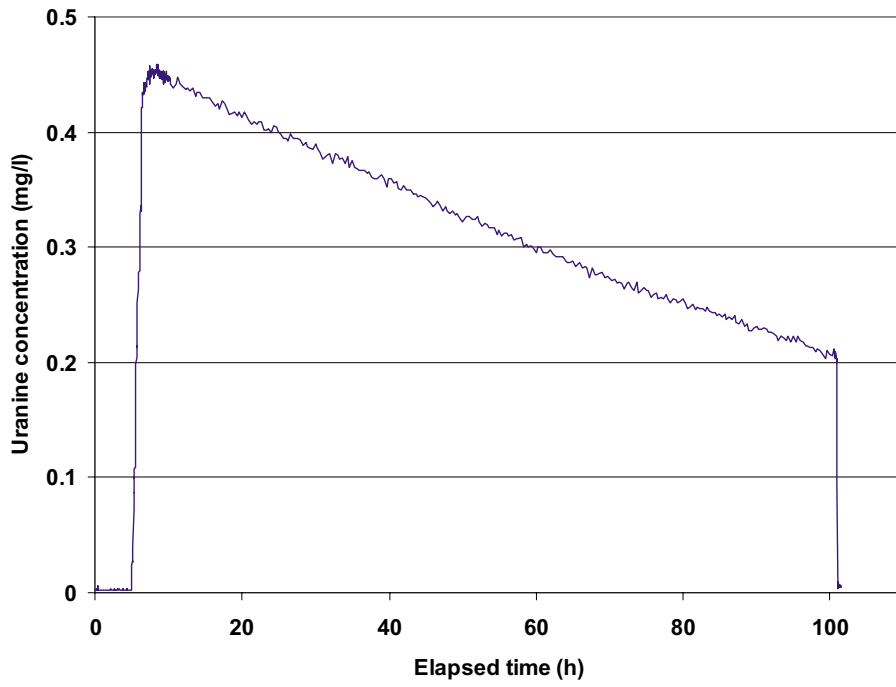


Figure 5-14. Dilution measurement in borehole KSH02, section 858.6–859.6 m.

KSH02 858.6–859.6 m

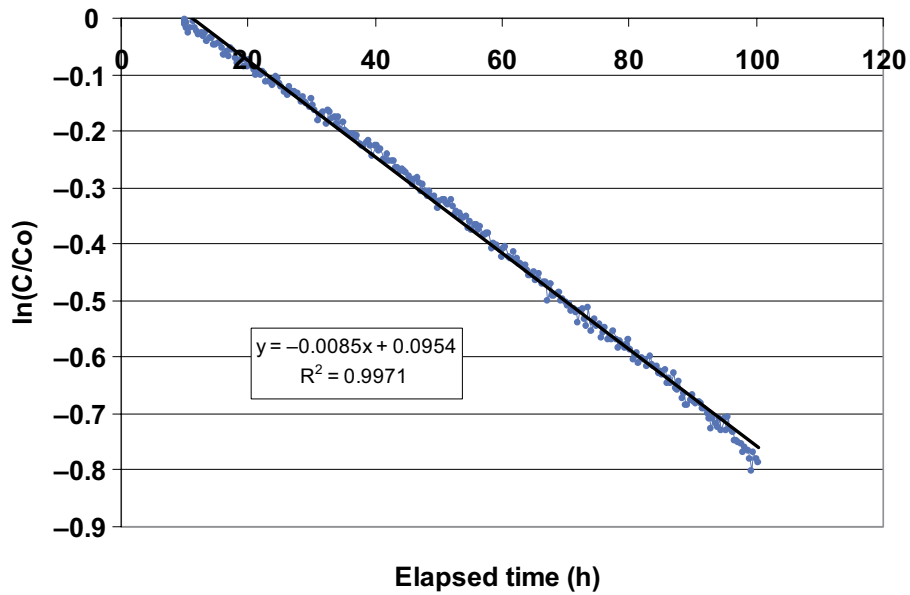


Figure 5-15. Linear regression best fit to data from dilution measurement in borehole KSH02, section 858.6–859.6 m.

5.1.7 KSH02, section 957.2–958.2 m

This dilution measurement was carried out in a single fracture with the dye tracer Uranine. The concentration versus time data is presented in Figure 5-16. Background concentration is close to zero. The Uranine tracer is injected in many small steps and after mixing it reaches a start concentration of 0.57 mg/l above background. Dilution is measured for about 100 hours. Thereafter the packers are deflated, but this and succeeding activities of the dilution measurement were not logged in this case. Hydraulic pressure shows no trend, only small diurnal pressure variations due to earth tidal effects (Appendix C5). It is obvious that the concentration versus time don't follow dilution according to theory, and the complete set of the $\ln(C/C_0)$ versus time data could not fit a straight line. For that reason the final evaluation was made on the last part of the dilution measurement, from 90 to 120 hours of elapsed time, where it is judged most stable conditions many hours from time of packer inflation. The correlation coefficient of the best fit line is $R^2 = 0.980$ (Figure 5-17). The groundwater flow rate, calculated from the best fit line, is 0.42 ml/min. Calculated hydraulic gradient is 0.086 and Darcy velocity 4.64×10^{-8} m/s. The hydraulic gradient is large and may be caused by a hydraulic shortcut or wrong estimates of correction factor, α , and/or the hydraulic conductivity as discussed in Chapter 5.1.3.

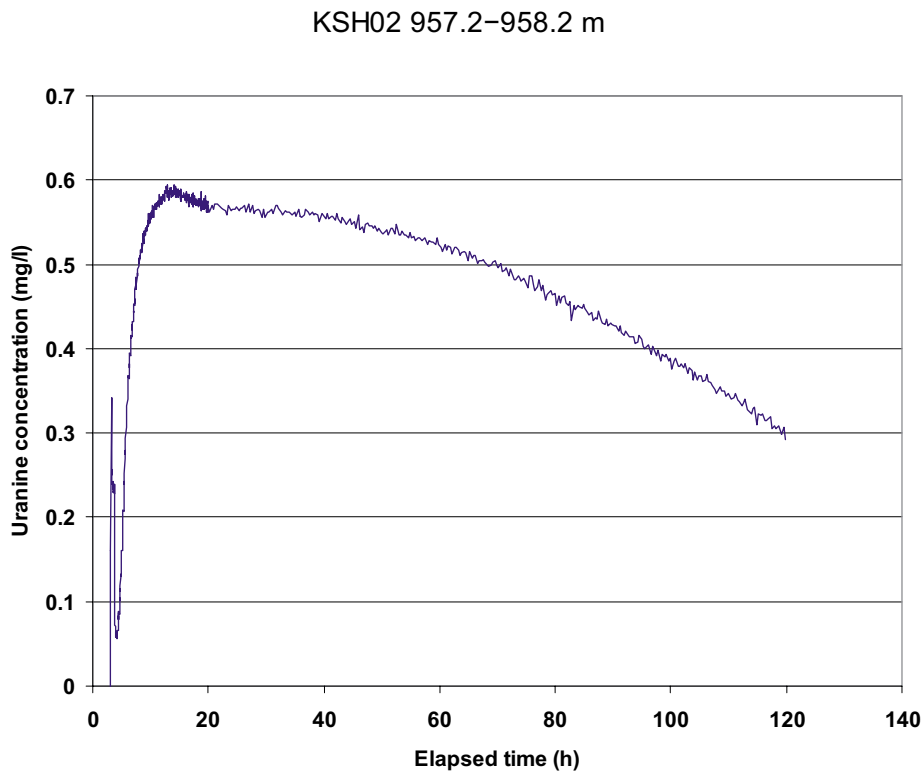


Figure 5-16. Dilution measurement in borehole KSH02, section 957.2–958.2 m.

KSH02 957.2–958.2 m

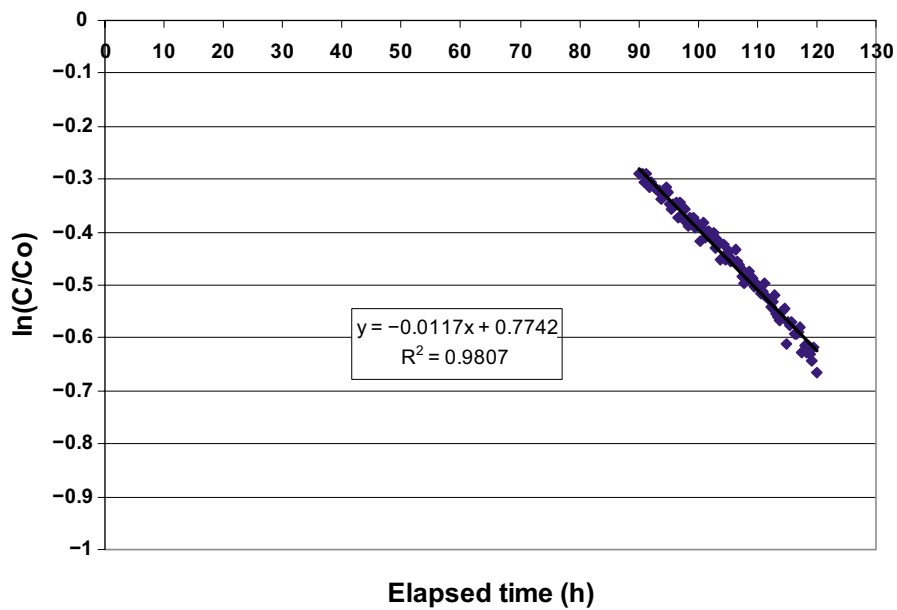


Figure 5-17. Linear regression best fit to data from dilution measurement in borehole KSH02, section 957.2–958.2 m.

5.1.8 Summary of dilution results

Calculated groundwater flow rate, Darcy velocity and hydraulic gradient from all dilution measurements carried out in boreholes KLX02 and KSH02 are presented in Table 5-1.

Table 5-1. Ground water flows, Darcy velocities and hydraulic gradients for all measured sections in boreholes KLX02 and KSH02.

Borehole	Test section (m)	T (m ² /s)*	Number of flowing fractures*	Q (ml/min)	Q (m ³ /s)	Darcy velocity (m/s)	Hydraulic gradient
KLX02	250.8–253.8	7.4E–6	3	2.81	4.68E–08	1.03E–07	0.042
KLX02	338.4–341.4	6.0E–7	3	0.42	6.97E–09	1.54E–08	0.077
KSH02	176.0–177.0	2.1E–7	1	0.65	1.09E–08	7.18E–08	0.347
KSH02	422.3–423.3	1.0E–6	1	0.19	3.25E–09	2.15E–08	0.021
KSH02	576.8–579.8	5.2E–7	Fracture zone with 3–4 flowing fractures	0.09	1.57E–09	3.44E–09	0.020
KSH02	858.6–859.6	1.3E–8	1	0.31	5.17E–09	3.41E–08	2.570
KSH02	957.2–958.2	5.4E–7	1	0.42	7.03E–09	4.64E–08	0.086

* From Difference flow logging /Rouhiainen, 2000; Rouhiainen and Pöllänen, 2003/.

The results show that the groundwater flow varies considerably in fractures and fracture zones during natural undisturbed conditions, with flow rates from 0.09 to 2.81 ml/min and Darcy velocities from 3.4×10^{-9} to 1.0×10^{-7} m/s. The highest flow rates are measured at shallow depth and flow rates decreases with depth, except for the single fractures at c 860 and 960 m depth, Figure 5-18. The high flow rate may be due to high hydraulic transmissivity in combination with a hydraulic shortcut where the measured fracture constitutes a hydraulic conductor between other fractures with different hydraulic heads. The Darcy velocity follows the same trend versus depth as the groundwater flow rate, Figure 5-19. A large portion of the measured fractures/fracture zones are within a small range of transmissivity, however correlation between flow rate and transmissivity is indicated in Figure 5-20. Hydraulic gradients, calculated according to the Darcy concept, are large in the single fractures at 176.0, 858.6, and 957.2 m depth. In the other measured fractures/fracture zones the hydraulic gradient is within the expected range. It is not clear if the large gradients in the single fractures are caused by local effects where the measured fracture constitutes a hydraulic conductor between other fractures with different hydraulic heads or due to wrong estimates of the correction factor, α , and/or the hydraulic conductivity of the fracture.

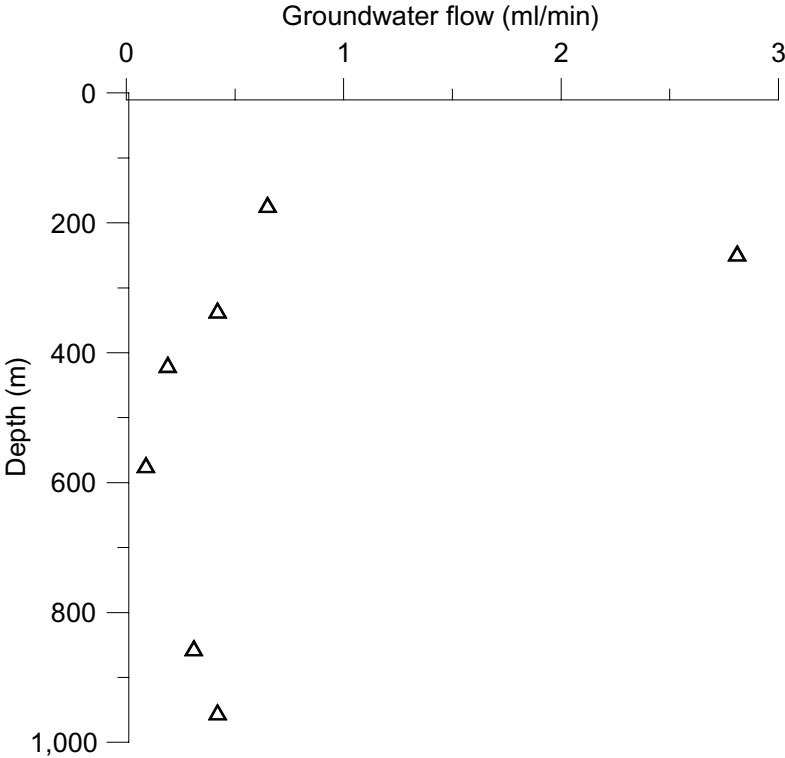


Figure 5-18. Groundwater flow versus depth during undisturbed natural hydraulic gradient conditions. Results from dilution measurements in fractures and fracture zones in boreholes KSH02 and KLX02.

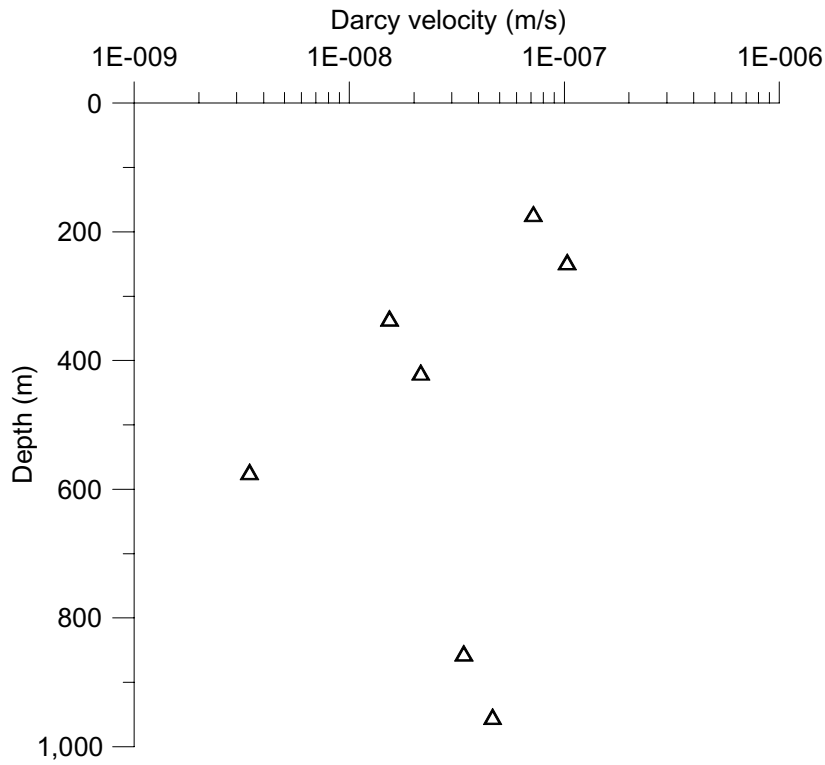


Figure 5-19. Darcy velocity versus depth during undisturbed natural hydraulic gradient conditions. Results from dilution measurements in fractures and fracture zones in boreholes KSH02 and KLX02.

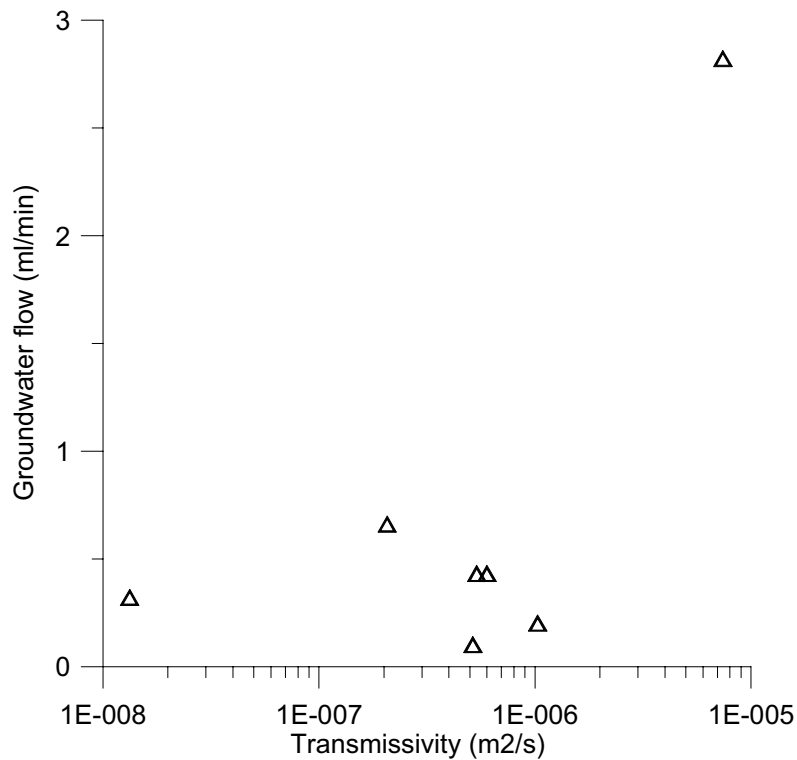


Figure 5-20. Groundwater flow versus transmissivity during undisturbed natural hydraulic gradient conditions. Results from dilution measurements in fractures and fracture zones in boreholes KSH02 and KLX02.

5.2 SWIW tests

5.2.1 Treatment of experimental data

The experimental data presented in this section have been corrected for background concentrations. Sampling times have been adjusted to account for residence times in injection and sampling tubing. Thus, time zero in all plots refers to when the fluid containing the tracer mixture start to enter the tested borehole section.

5.2.2 Tracer recovery breakthrough in KSH02, 422.3–423.3 m

Durations and flows for the various experimental phases are summarised in Table 5-2. In this case, two waiting phases and a second chaser injection phase occurred due to pump malfunction. During repair work, the packers were released which resulted in an outflow from the borehole into the tested formation. The magnitude of the outflow during this period was calculated from pressure measurement and transmissivity estimates and, thus, not measured directly. The extra waiting phases occurred during packed-off conditions and should not have resulted in any significant flows.

The experimental breakthrough curves from the recovery phase for Uranine and Cesium, respectively, are shown in Figures 5-21a and 5-21b. The time coordinates are corrected for residence time in the various tubing, as described above.

Normalised breakthrough curves (concentration divided by total injected tracer mass) for Uranine and Cesium, respectively, are plotted in Figure 5-22. The figure indicates similar tracer behaviour as in section 576.8–576.9 m, Figure 5-25, but with an even more pronounced retardation effect for Cesium.

Estimated tracer recovery at the last sampling time amounts to 86.2% and 40.7% for Uranine and Cesium, respectively. Final recovery values, i.e. that would have resulted if pumping had been carried out until tracer background values, are difficult to estimate from the experimental curves. However, as for section 576.8–579.8, plausible visual extrapolations of the curves do not clearly show that the tracer recovery would be different between the two tracers. Thus, for the subsequent model evaluation, it is assumed that tracer recovery is the same for both tracers.

Table 5-2. Durations (hours) and fluid flows (L/h) during various experimental phases for section 422.3–423.3 m.

Phase	Start (h)	Stop (h)	Volume (L)	Average flow (L/h)	Cumulative injected volume (L)
Pre-injection	-1.86	0	27.9	15.0	–
Tracer injection	0	0.95	14.25	15.0	14.25
Chaser injection 1	0.95	13.12	163.1	13.4	177.35
Waiting phase 1	13.12	15.17	0	0	177.35
Chaser injection 2	15.17	63.50	26.6 ¹	0.55 ¹	203.95
Waiting phase 2	64.50	65.2	0	0	203.95
Withdrawal (Recovery)	65.2	182.98	1,766.7	15.0	

¹) This value is calculated using an estimate of transmissivity based on differential flow logging and hydraulic injection tests and measured pressure difference in the fracture and in the open borehole at the location of the fracture at 422 m.

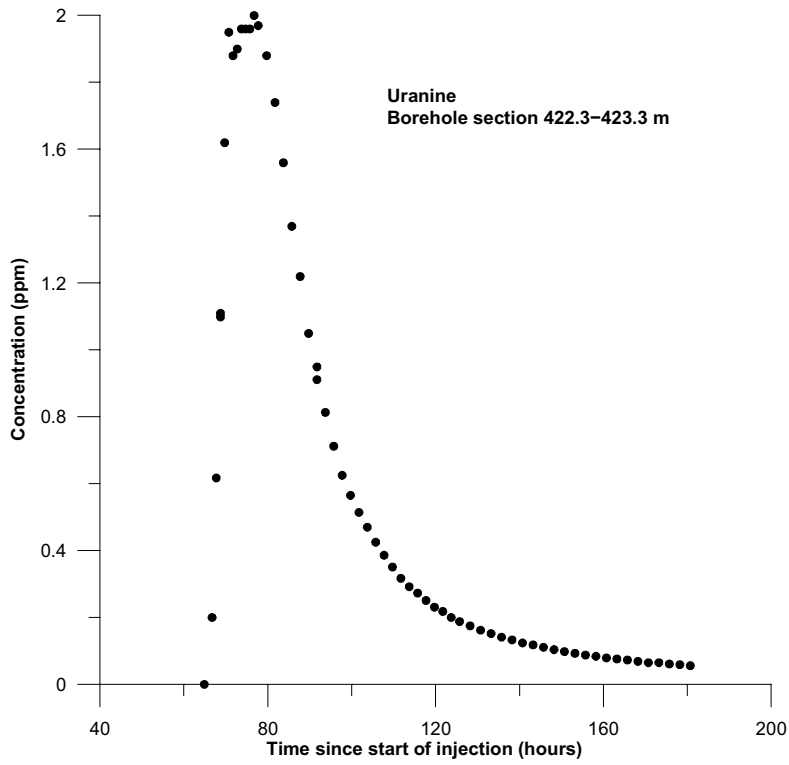


Figure 5-21a. Withdrawal (recovery) phase breakthrough curve for Uranine in section 422.3–423.3 m in borehole KSH02.

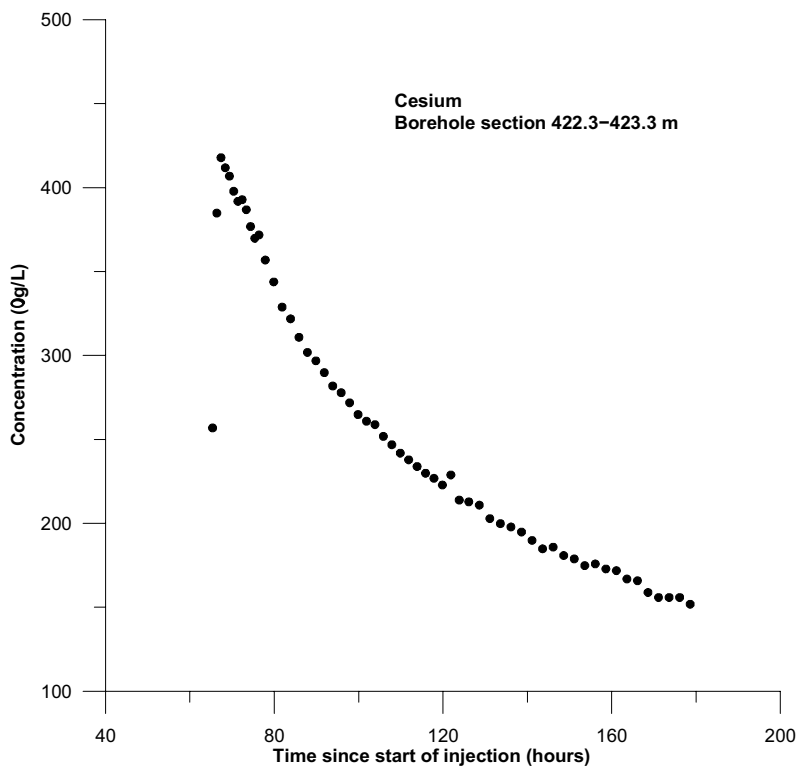


Figure 5-21b. Withdrawal (recovery) phase breakthrough curve for Cesium in section 422.3–423.3 m in borehole KSH02.

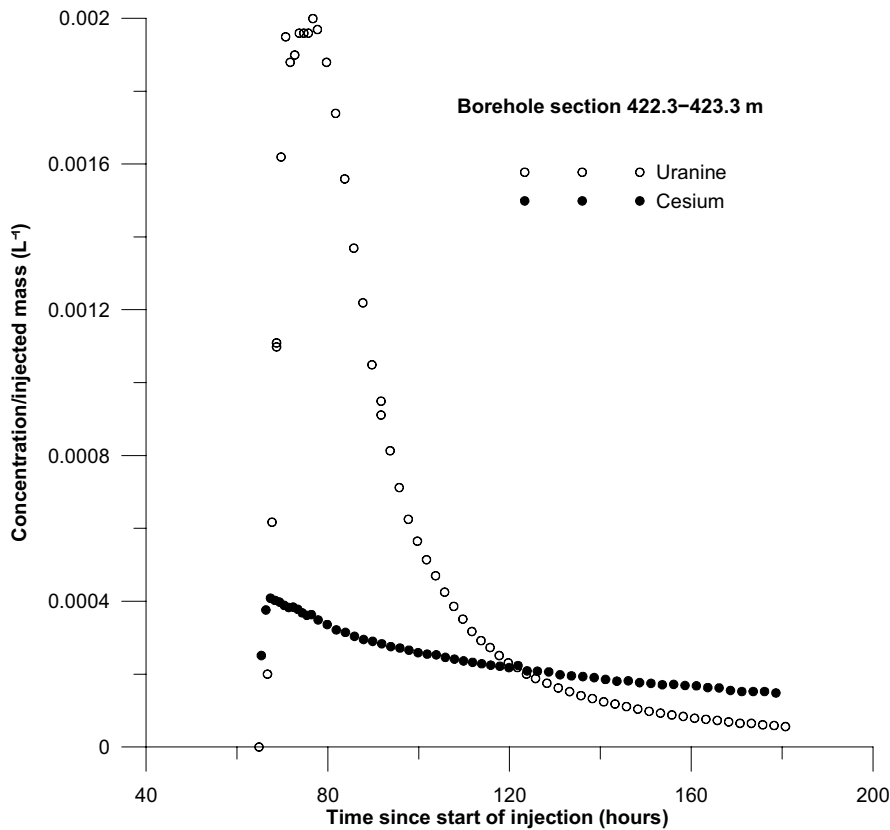


Figure 5-22. Normalised withdrawal (recovery) phase breakthrough curves for Uranine and Cesium in section 422.3–423.3 m.

5.2.3 Model evaluation KSH02, 422.3–423.3 m

The model simulations were carried out assuming negligible hydraulic background gradient, i.e. purely radial flow. The simulated times and flows in the various experimental phases are given in Table 5-2. This section is considered to be dominated by a single fracture. In the simulation model, the flow zone is approximated by a 0.1 m thick fracture zone.

For a given regression run, estimation parameters were longitudinal dispersivity (α_L) and a linear retardation factor (R), while the porosity is given a fixed value. Regression was carried for five different values of porosity: 0.002, 0.005, 0.01, 0.02 and 0.05. For all cases, the fit between model and experimental data is similar.

The results of the fitting for different values of assumed porosity are given in Table 5-3.

The fit between simulation model and experimental for Uranine is similar to section 576.8–579.8 m, with a discrepancy in the tail of the curve. The fit for Cesium is, however, not so good in this case. The simulation model can not be considered to fit the Cesium data well in any part of the recovery breakthrough curve. All of the regression runs result in very large retardation factors, about 950–1,000. A clear indication that such estimates of R are significantly too high is that the model curve prior to the recovery phase does not at all reach sufficiently low levels to be able to include the first two points of the ascending part of the Cesium curve. In this case, it may be possible inclusion of other processes, such as diffusion and sorption in the rock matrix/fracture coatings, would give a better fit of experimental data. Because of the prolonged experimental times due to the extra chaser and waiting phases, time-dependent processes could potentially be more influential in this case compared with section 576.8–579.8 m.

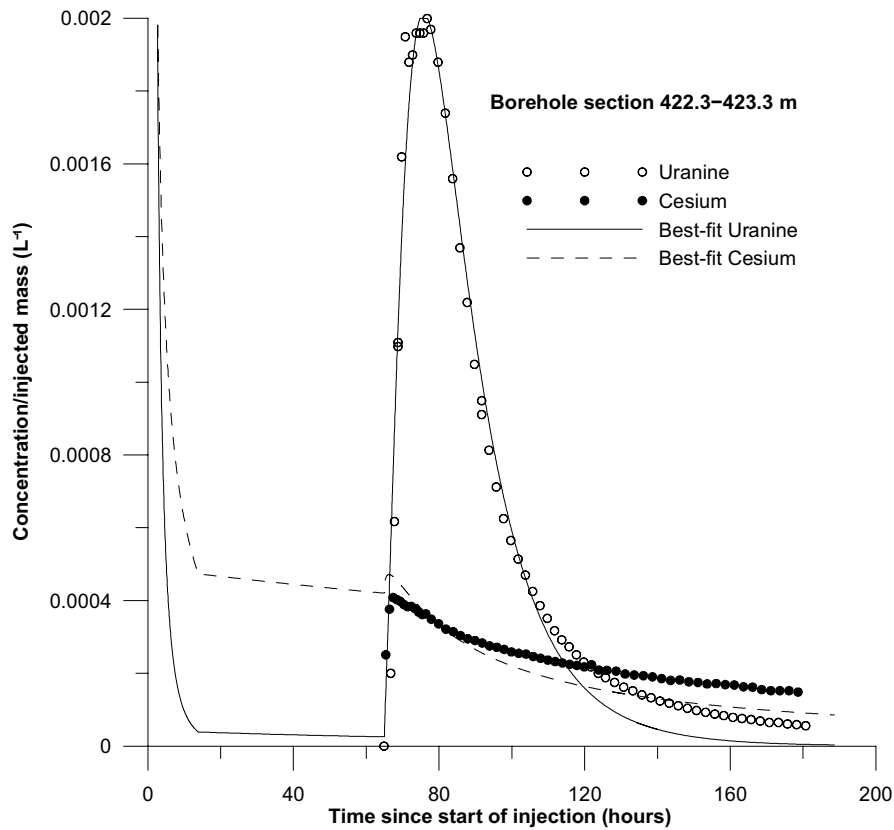


Figure 5-23. Example of simultaneous fitting of Uranine and Cesium for section 422.3–423.3 m in borehole KSH02.

Table 5-3. Results of model fitting for section 422.3–423.3 in borehole KSH02. Coefficient of variation values are given within parenthesis.

Porosity (fixed)	a_L (estimated)	R (estimated)
0.002	2.50 (0.05)	1,001 (0.20)
0.005	1.53 (0.04)	978 (0.16)
0.01	1.08 (0.04)	975 (0.16)
0.02	0.57 (0.04)	969 (0.16)
0.05	0.48 (0.04)	952 (0.16)

5.2.4 Tracer recovery breakthrough in KSH02, 576.8–579.8 m

Durations and flows for the various experimental phases are summarised in Table 5-4.

Table 5-4. Durations (hours) and fluid flows during various experimental phases for section 576.8–579.8 m in borehole KSH02.

Phase	Start (h)	Stop (h)	Volume (L)	Average flow (L/h)	Cumulative injected volume (L)
Pre-injection	-2.63	0	35.2	13.4	–
Tracer injection	0	0.83	10.8	13.0	10.8
Chaser injection	0.83	15.3	163.5	11.3	174.3
Withdrawal (Recovery)	15.3	110.3	1,634	17.2	

The experimental breakthrough curves from the withdrawal (recovery) phase for Uranine and Cesium, respectively, are shown in Figures 5-24a and 5-24b. The time coordinates are corrected for residence time in the tubing, as described above.

For a number of the Uranine samples from section 576.8–579.8 m, chemical precipitation/miss colouring occurred that resulted in apparently erroneous concentration values. The cause of this process is not known, but similar transition of Uranine samples has previously occurred occasionally in tracer tests at depth in the Äspö Hard Rock Laboratory. Those values have been omitted in the plots presented in this section.

Normalised breakthrough curves (concentration divided by total injected tracer mass) for Uranine and Cesium, respectively, are plotted in Figure 5-25. The figure shows that the two tracers behave in different ways, presumably caused by different sorption properties. Qualitatively, the breakthrough curves appear to approximately conform to what would be expected from a SWIW test using tracers of different sorption properties. The considerable difference between the two curves can also be seen as an indication of a relatively strong sorption effect.

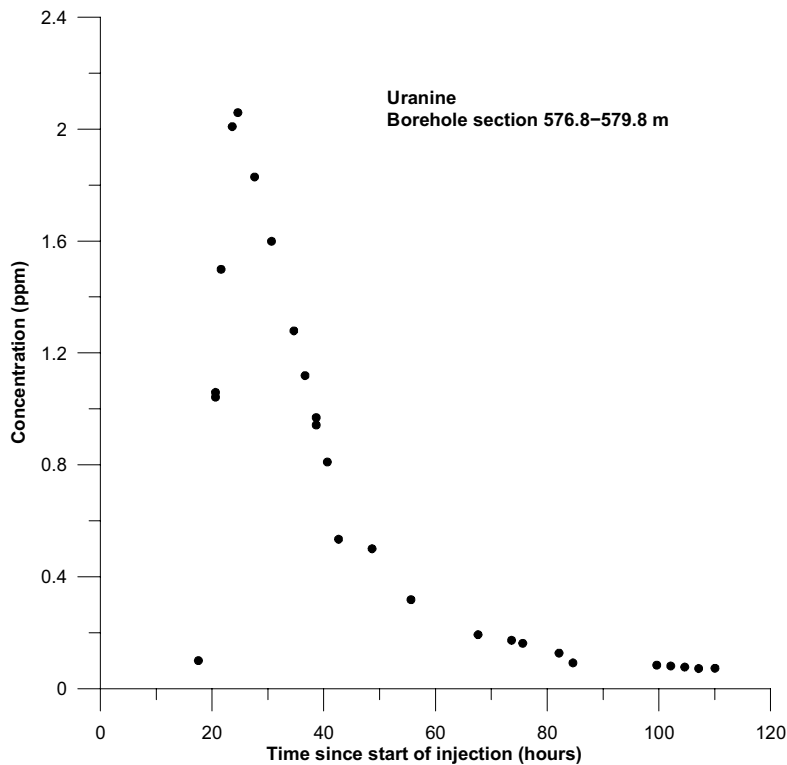


Figure 5-24a. Withdrawal (recovery) phase breakthrough curve for Uranine in section 576.8–579.8 m in borehole KSH02.

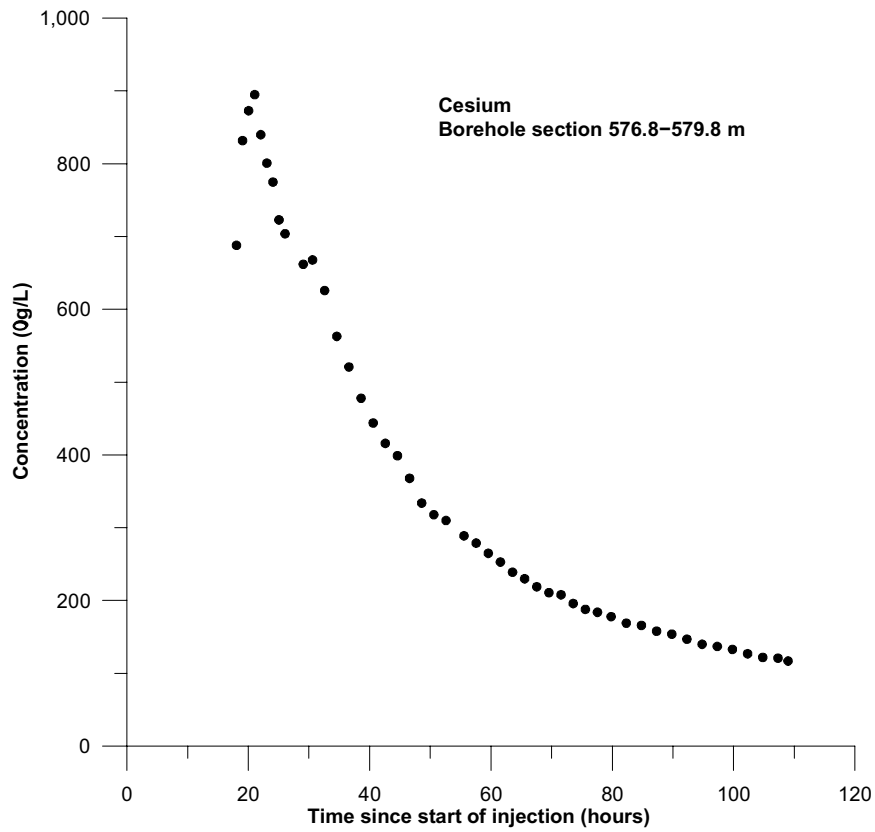


Figure 5-24b. Recovery phase breakthrough curve for Cesium in section 576.8–579.8 m in borehole KSH02.

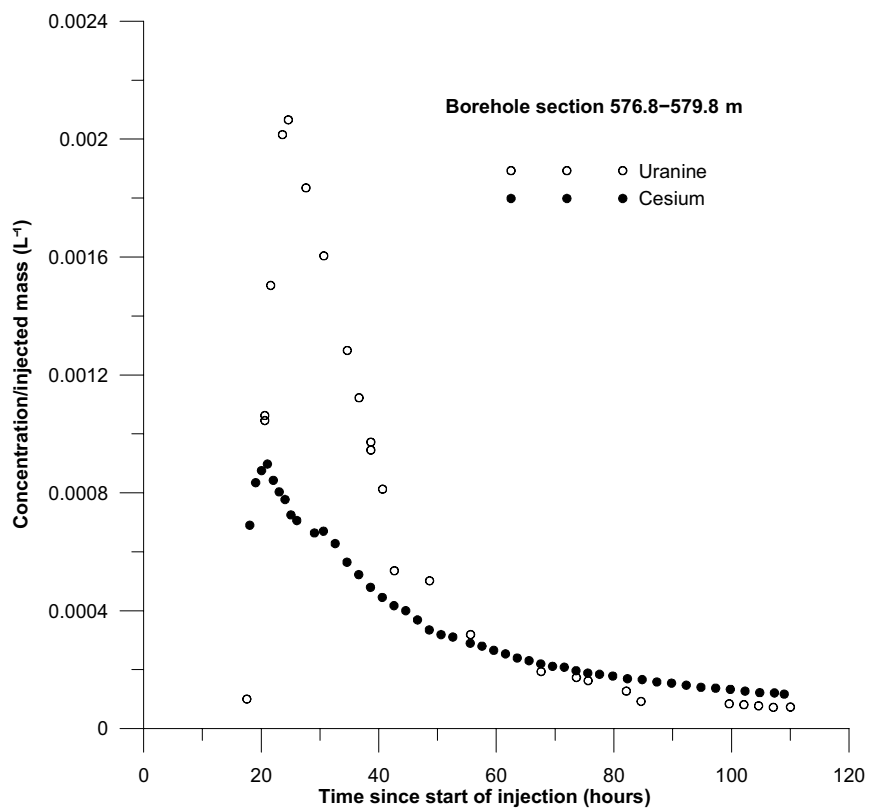


Figure 5-25. Normalised withdrawal (recovery) phase breakthrough curves for Uranine and Cesium in section 576.8–579.8 m in borehole KSH02.

The tracer recovery from the withdrawal phase pumping is rather difficult to estimate from the experimental breakthrough curves, because the tailing parts appear to continue beyond the last sampling time. A preliminary estimation of recovery from the experimental breakthrough curves at the last sampling time yields values of 80.5 and 51.6% for Uranine and Cesium, respectively. These estimates are based on the average flow rate during the entire recovery phase.

Final recovery values, i.e. that would have resulted if pumping had been carried out until tracer background values, are difficult to estimate from the experimental curves. However, plausible visual extrapolations of the curves do not clearly indicate that the tracer recovery would be different between the two tracers. Thus, for the subsequent model evaluation, it is assumed that tracer recovery is the same for both tracers.

5.2.5 Model evaluation KSH02, 576.8–579.8 m

The model simulation was carried with the same assumptions as for section 422.3–423.3 m. The simulated times and flows in the various experimental phases are given in Table 5-4. This section consists of several fractured parts; one altered zone of about 0.1 m and 2–3 additional single fractures. An example of a model fit is shown in Figure 5-11. The results of the fitting for different values of assumed porosity are given in Table 5-5.

The model fits to the experimental breakthrough curves are generally fairly good. The main discrepancy is observed for the tailing part of the Uranine curve. There is a similar tendency for the Cesium curve, but much less than for Uranine. All of the regression runs (Table 5-5) resulted in similar values of the retardation coefficient, while the estimated values of the longitudinal dispersivity are strongly dependent on the assumed porosity value. Both of these observations are consistent with prior expectations of the relationships between parameters in a SWIW test /Nordqvist and Gustafson, 2002/.

The estimated value of the R for Cesium indicates a strong sorption. The values of R agree approximately with values from cross-hole tests, obtained using similar transport models (advection-dispersion and linear sorption). /Winberg et al. 2000/ reported a value of R = 69 for Cesium, while a value of R = 140 was reported by /Andersson et al. 1999/.

Table 5-5. Results of model fitting for section 576.8–579.8 in borehole KSH02. Coefficient of variation values (estimation standard error divided by the estimated value) are given within parenthesis.

Porosity (fixed)	a_L (estimated)	R (estimated)
0.002	1.77 (0.06)	90.8 (0.16)
0.005	1.14 (0.05)	87.5 (0.14)
0.01	0.81 (0.05)	87.4 (0.14)
0.02	0.57 (0.05)	87.2 (0.14)
0.05	0.36 (0.05)	86.8 (0.14)

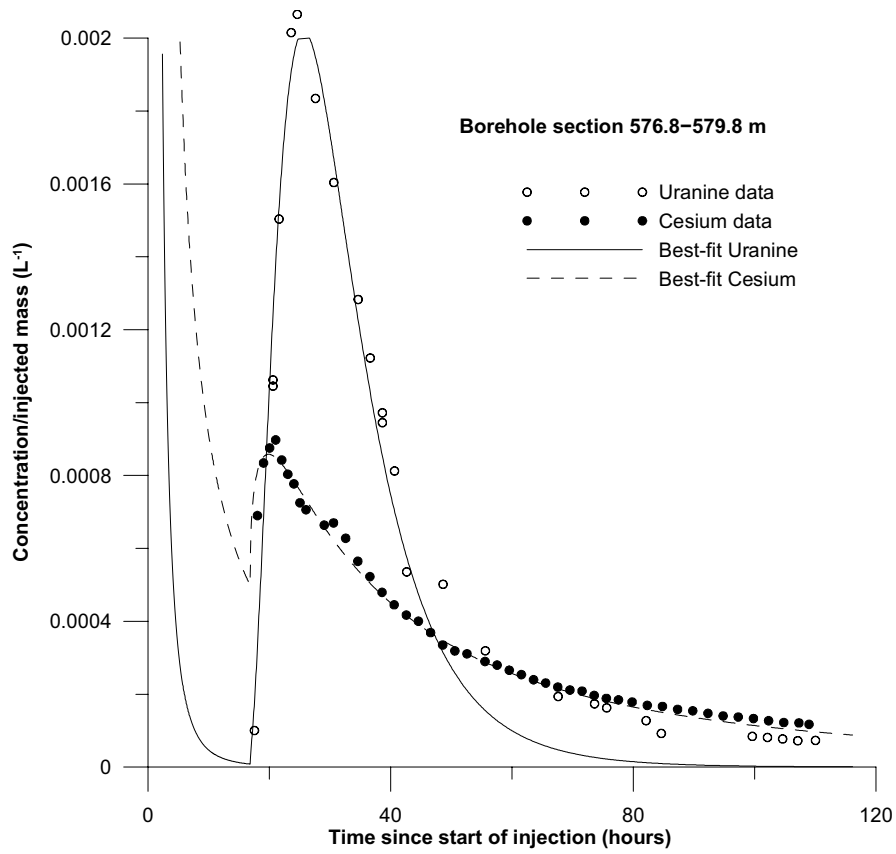


Figure 5-26. Example of simultaneous fitting of Uranine and Cesium for section 576.8–579.8 m in borehole KSH02.

6 Discussion and conclusions

The results of the dilution measurements in boreholes KSH02 and KLX02 show that the groundwater flow varies considerably in fractures and fracture zones during natural undisturbed conditions, although the flow rates and Darcy velocities decrease with depth. The exceptions are two single fractures at c 860 and 960 m depth. The high flow rates may be due to high hydraulic transmissivity in combination with a hydraulic shortcut where the measured fractures constitute hydraulic conductors to other fractures having different hydraulic heads. It should also be considered that in fractured rock, during natural hydraulic conditions, the groundwater flow in fractures and fracture zones to a large extent is governed by the direction of the large-scale hydraulic gradient relative to the strike and dip of the conductive fractures and zones.

Groundwater flows and Darcy velocities calculated from dilution measurements in boreholes KSH02 and KLX02 are within the range that can be expected out of experience from previously performed dilution measurements under natural gradient conditions at other sites in Swedish crystalline rock (Gustafsson and Andersson, 1991/ Gustafsson and Morosini, 2002/). In KSH02 and KLX02 hydraulic transmissivity ranged within $T = 1.3 \times 10^{-8} - 7.4 \times 10^{-6} \text{ m}^2/\text{s}$, flow rate ranged from 0.09 to 2.81 ml/min and Darcy velocity from 3.4×10^{-9} to $1.0 \times 10^{-7} \text{ m/s}$ ($2.9 \times 10^{-4} - 8.6 \times 10^{-3} \text{ m/d}$). (Gustafsson and Morosini, 2002/ reported two dilution measurements performed at the Ävrö site, located close to Simpevarp and Laxemar areas. The dilution measurement carried out in a shallow 70–80 m highly conductive fracture zone in borehole KAV01 with $T = 1.0 \times 10^{-5} \text{ m}^2/\text{s}$ showed a groundwater flow rate of 31.5 ml/min and Darcy velocity $4.7 \times 10^{-7} \text{ m/s}$ (0.04 m/d). A minor fracture at 433.4–435.4 m depth in KAV01 with $T = 2.0 \times 10^{-9} \text{ m}^2/\text{s}$ showed practically no dilution and very low flow, 0.008 ml/min and corresponding Darcy velocity $6.2 \times 10^{-10} \text{ m/s}$ ($5.5 \times 10^{-5} \text{ m/d}$).

The SWIW tests in the two sections described here have resulted in high-quality tracer breakthrough data. Experimental conditions (flows, times, events, etc) are well known and documented, which provides a good basis for further evaluation of the data if desired.

The results show smooth breakthrough curves without apparent irregularities or excessive experimental noise in both tested sections. The most significant result is that there is a very clear effect of retardation/sorption of Cesium in both tests. Thus, it has been demonstrated that tracer retardation can be tested with field SWIW tests.

The model evaluation was made using a radial flow model with advection, dispersion and linear equilibrium sorption as transport processes. It is important that experimental conditions (times, flows, injection concentration, etc) are incorporated accurately in the simulations, otherwise artefacts of erroneous input may occur in the simulated results. This may be regarded as a typical preliminary approach for evaluation of a SWIW test where sorbing tracers are used. Background flows were in this case assumed, supported by dilution measurement results, to be insignificant.

The estimated value of the retardation factor for Cesium in section 576.8–579.8 m, $R = 90$ indicates a strong sorption. The value of R agrees approximately with values from cross-hole tests, obtained using similar transport models (advection-dispersion and linear sorption). (Winberg et al. 2000/ reported a value of $R = 69$ for Cesium, while a value of $R = 140$ was reported by (Andersson et al. 1999/). The estimated value of R for section 422.3–423.3 m was much larger, on the order of 1,000. However, due to a systematic discrepancy in the fitted breakthrough curve, such a large value was not deemed relevant. Instead, there may be other processes that need to be included, such as diffusion into stagnant zones/matrix.

7 References

Andersson P, 1995. Compilation of tracer tests in fractured rock. SKB Report PR 25-95-05.

Andersson P, Wass E, Byegård J, Johansson H, Skarnemark G, 1999. Äspö Hard Rock Laboratory. True 1st stage tracer programme. Tracer test with sorbing tracers. Experimental description and preliminary evaluation. SKB Report IPR-99-15.

Carlsten S, Strähle A, Ludvigson J-E, 2001. Conductive fracture mapping. A study on the correlation between borehole TV- and radar images and difference flow logging results in borehole KLX02. SKB R-01-48. Svensk Kärnbränslehantering AB.

Gustafsson E, 2002. Bestämning av grundvattenflödet med utspädningsteknik - Modifiering av utrustning och kompletterande mätningar. SKB R-02-31 (in Swedish). Svensk Kärnbränslehantering AB.

Gustafsson E, Andersson P, 1991. Groundwater flow conditions in a low-angle fracture zone at Finnsjön, Sweden. *Journal of Hydrology*, Vol 126, pp 79–111. Elsevier, Amsterdam.

Gustafsson E, Morosini M, 2002. In-situ groundwater flow measurements as a tool for hardrock site characterisation within the SKB programme. *Norges geologiske undersøkelse. Bulletin 439*, 33–44.

Halevy E, Moser H, Zellhofer O, Zuber A, 1967. Borehole dilution techniques – a critical review. In: *Isotopes in Hydrology, Proceedings of a Symposium, Vienna 1967, IAEA, Vienna*, pp 530–564.

Nordqvist R, Gustafsson E, 2002. Single-well injection-withdrawal tests (SWIW). Literature review and scoping calculations for homogeneous crystalline bedrock conditions. SKB R-02-34. Svensk Kärnbränslehantering AB.

Nordqvist R, Gustafsson E, 2004. Single-well injection-withdrawal tests (SWIW). Investigation of evaluation aspects under heterogeneous crystalline bedrock conditions. SKB R-04-57. Svensk Kärnbränslehantering AB.

Rhén I, Forsmark T, Gustafson G, 1991. Transformation of dilution rates in borehole sections to groundwater flow in the bedrock. Technical note 30. In: Liedholm M. (ed) 1991. SKB-Äspö Hard Rock Laboratory, Conceptual Modeling of Äspö, technical Notes 13-32. General Geological, Hydrogeological and Hydrochemical information. Äspö Hard Rock Laboratory Progress Report PR 25-90-16b.

Rouhiainen P, 2000. Äspö Hard Rock Laboratory. Difference flow measurements in borehole KLX02 at Laxemar. SKB Report IPR-01-06.

Rouhiainen P, Pöllänen J, 2003. Oskarshamn site investigation. Difference flow measurements in borehole KSH02 at Simpevarp. SKB P-03-110. Svensk Kärnbränslehantering AB.

SKB 2001a. Site investigations. Investigation methods and general execution programme. SKB TR-01-29. Svensk Kärnbränslehantering AB.

SKB 2001b. Geovetenskapligt program för platsundersökning vid Simpevarp. SKB R-01-44 (in Swedish). Svensk Kärnbränslehantering AB.

Voss C I, 1984. SUTRA – Saturated-Unsaturated Transport. A finite element simulation model for saturated-unsaturated fluid-density-dependent ground-water flow with energy transport or chemically-reactive single-species solute transport. U.S. Geological Survey Water-Resources Investigations Report 84-4369.

Wacker P, Berg C, 2004. Oskarshamn site investigation. Water sampling in KSH02A. Summary of water sampling analysis in connection with Pipe String System (PSS) and Single Well Injection Withdrawal (SWIW) measurements. SKB P-04-281. Svensk Kärnbränslehantering AB.

Winberg A, Andersson P, Hermansson J, Byegård J, Cvetkovic V, Birgersson L, 2000. Äspö Hard Rock Laboratory. Final report of the first stage of the tracer retention understanding experiment. SKB TR-00-07. Svensk Kärnbränslehantering AB.

Borehole data KLX02 and KSH02

SICADA – Information about KLX02.

Title	Value				
	Information about cored borehole KLX02 (2004-02-10).				
Borhole length (m):	1,700.500				
Reference level:	TOC				
Drilling Period(s):	From Date	To Date	Secup (m)	Seclow (m)	Drilling Type
	1992-08-15	1992-09-05	0.000	202.950	Core drilling
	1992-10-15	1992-11-29	202.950	1,700.500	Core drilling
Starting point coordinate:	Length (m)	Northing (m)	Easting (m)	Elevation	Coord System
	0.000	6,366,768.985	1,549,224.090	18.400	RT90–RHB70
Angles:	Length (m)	Bearing	Inclination (– = down)		
	0.000	9.119	–85.000		
Borehole diameter:	Secup (m)	Seclow (m)	Hole Diam (m)		
	0.400	3.000	0.340		
	3.000	200.800	0.215		
	200.800	201.000	0.165		
	201.000	202.950	0.092		
	202.950	1,700.500	0.076		
Casing diameter:	Secup (m)	Seclow (m)	Case In (m)	Case Out (m)	
	0.000	3.000	0.250		
	3.000	200.800	0.183	0.194	
	200.800	202.950	0.077	0.084	

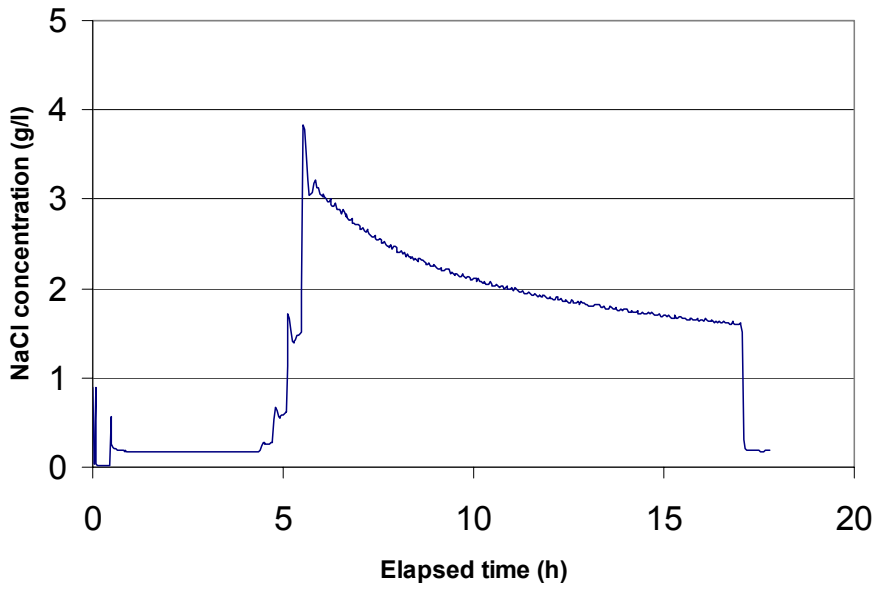
SICADA – Information about KSH02.

Title	Value				
	Information about cored borehole KSH02 (2004-11-04).				
Borhole length (m):	1,001.11				
Starting point coordinate:	Length (m)	Northing (m)	Easting (m)	Elevation	Coord System
	0.000	6,365,658.327	1,551,528.934	5.482	RT90–RHB70
Angles:	Length (m)	Bearing	Inclination	(– = down)	
	0.000	330.683	–85.685		
Borehole diameter:	Secup (m)	Seclow (m)	Hole Diam (m)		
	0.100	3.550	0.390		
	3.550	16.780	0.350		
	16.780	65.850	0.248		
	65.850	80.000	0.086		
	80.000	1,001.110	0.076		
Casing diameter:	Secup (m)	Seclow (m)	Case In (m)	Case Out (m)	
	0.000	65.360	0.200	0.208	
	0.100	16.780	0.265	0.273	
	65.360	80.000	0.080	0.084	

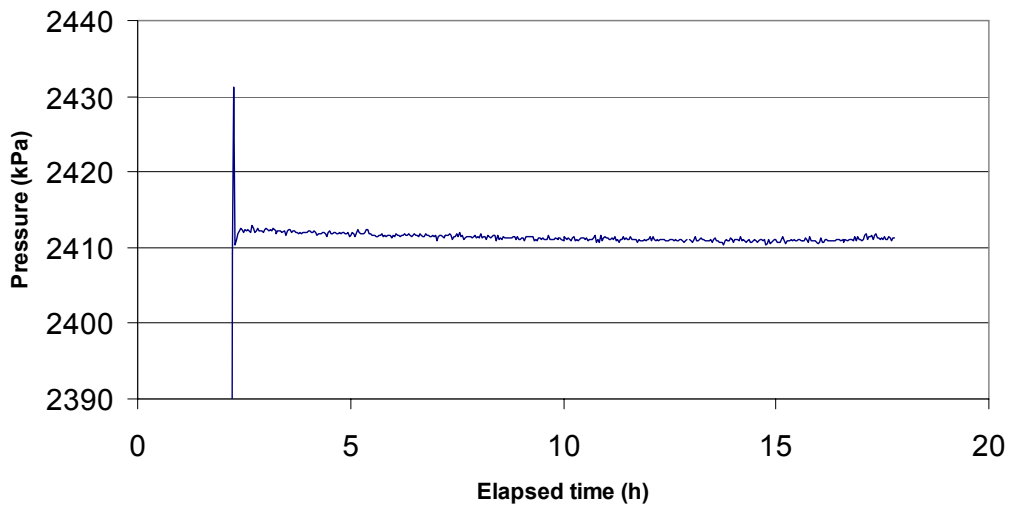
Dilution measurement KLX02

Dilution measurement KLX02 250.8–253.8 m

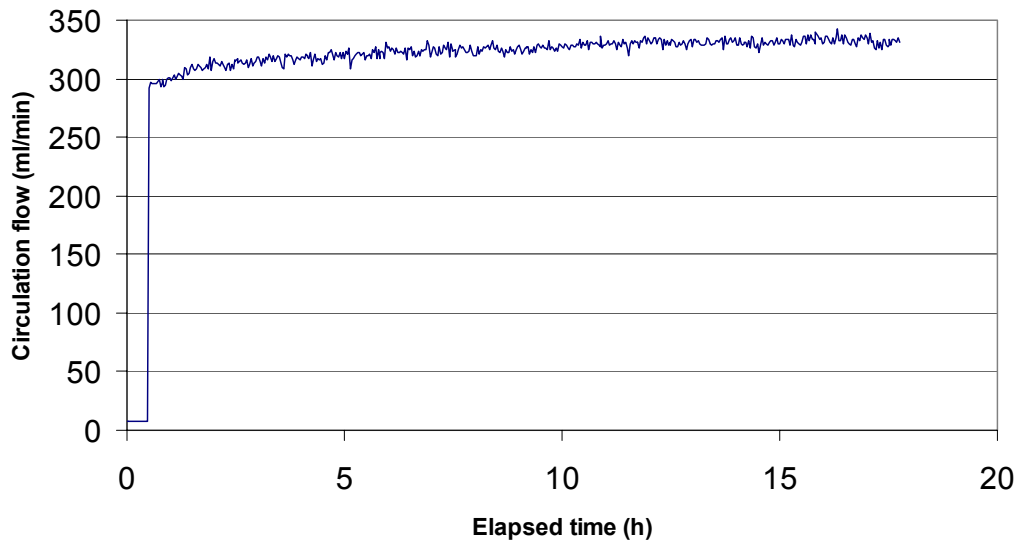
KLX02 250.8 - 253.8 m



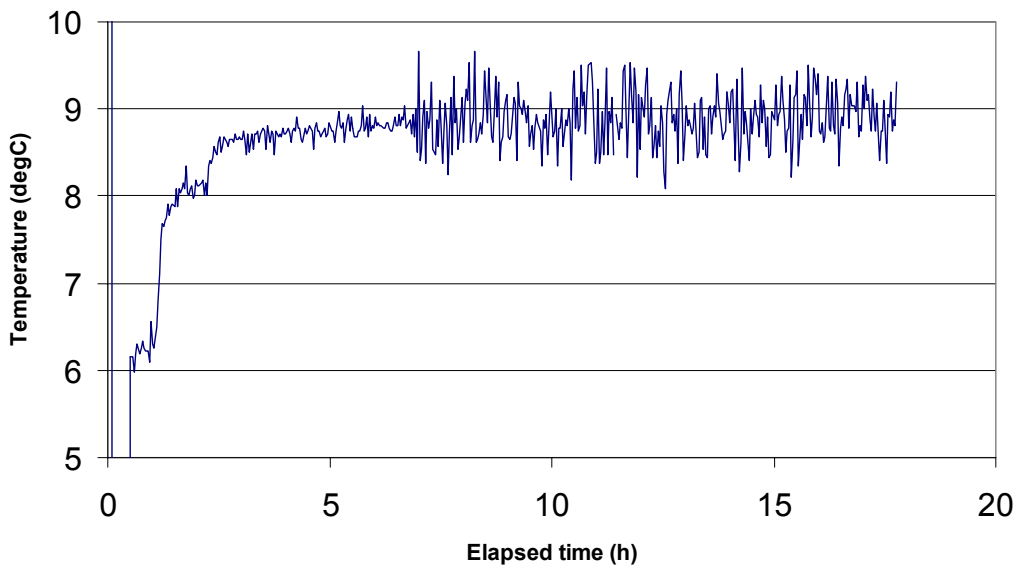
KLX02 250.8 - 253.8 m



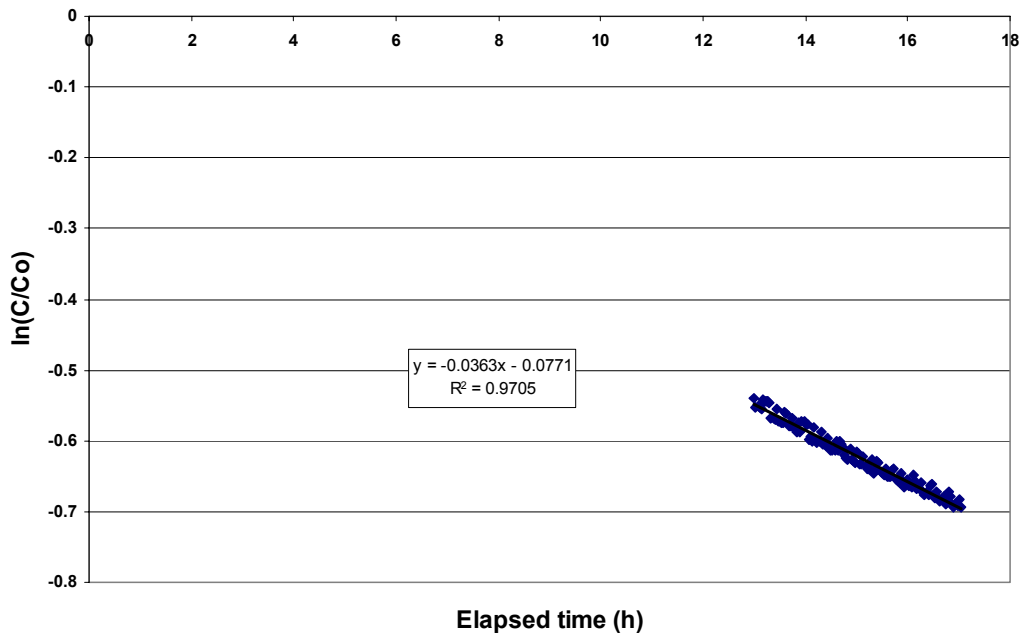
KLX02 250.8 - 253.8 m



KLX02 250.8 - 253.8 m



KLX02 250.8 - 253.8 m

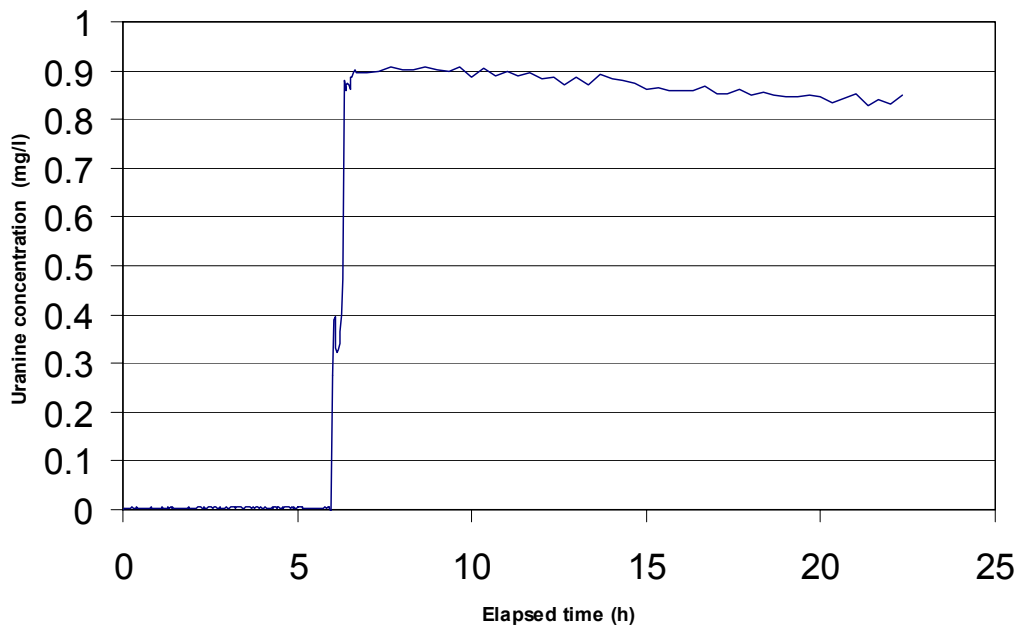


Part of dilution curve (h)	V (ml)	$\ln(C/C_0)/t$	Q (ml/h)	Q (ml/min)	Q (m ³ /s)	R2-value
13-17	4,645	-0.0363	168.61	2.81	4.68E-08	0.9705

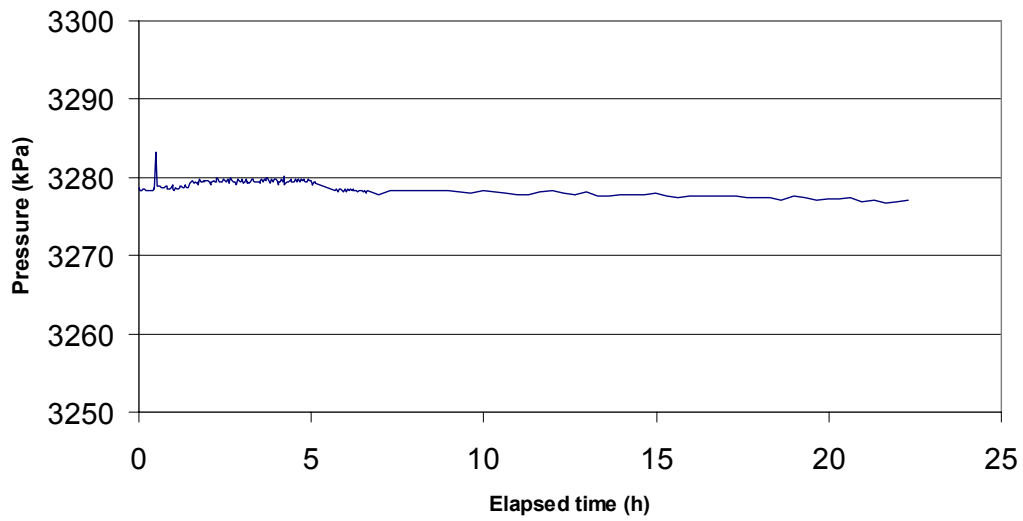
Part of dilution curve (h)	K (m/s)	Q (m ³ /s)	A (m ²)	v (m/s)	l
13-17	2.47E-06	4.68E-08	0.454	1.03E-07	4.17E-02

Dilution measurement KLX02 338.4–341.4 m

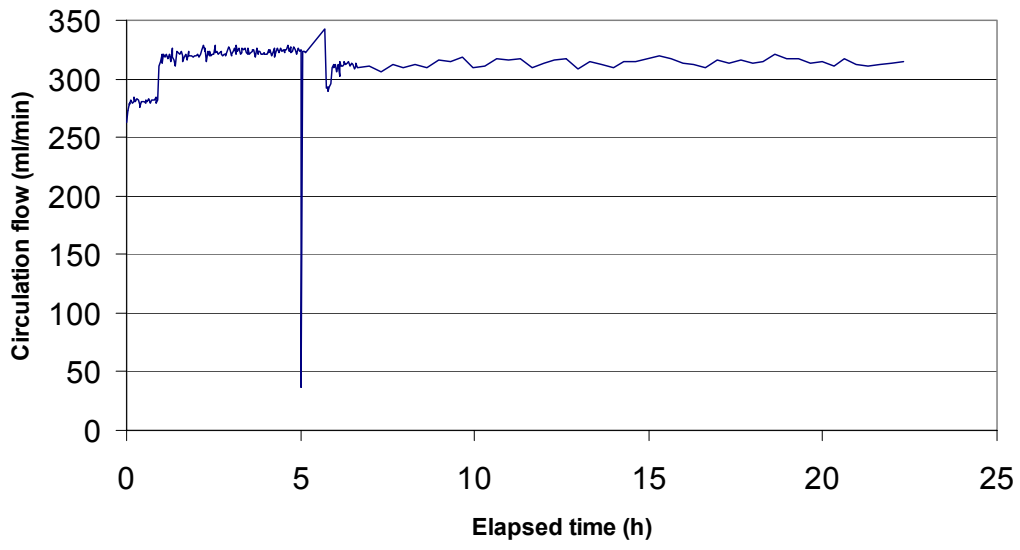
KLX02 338.4 - 341.4 m



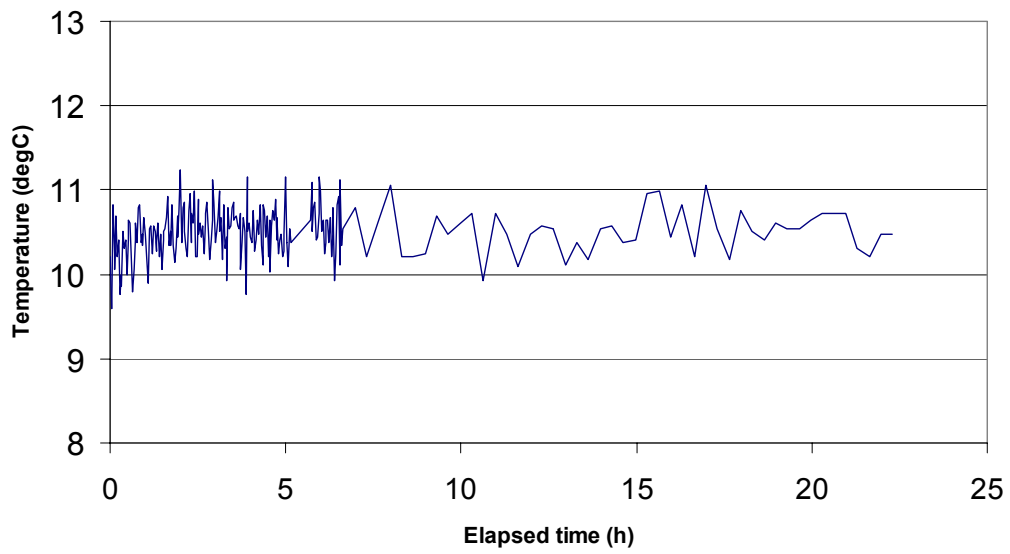
KLX02 338.4 - 341.4 m



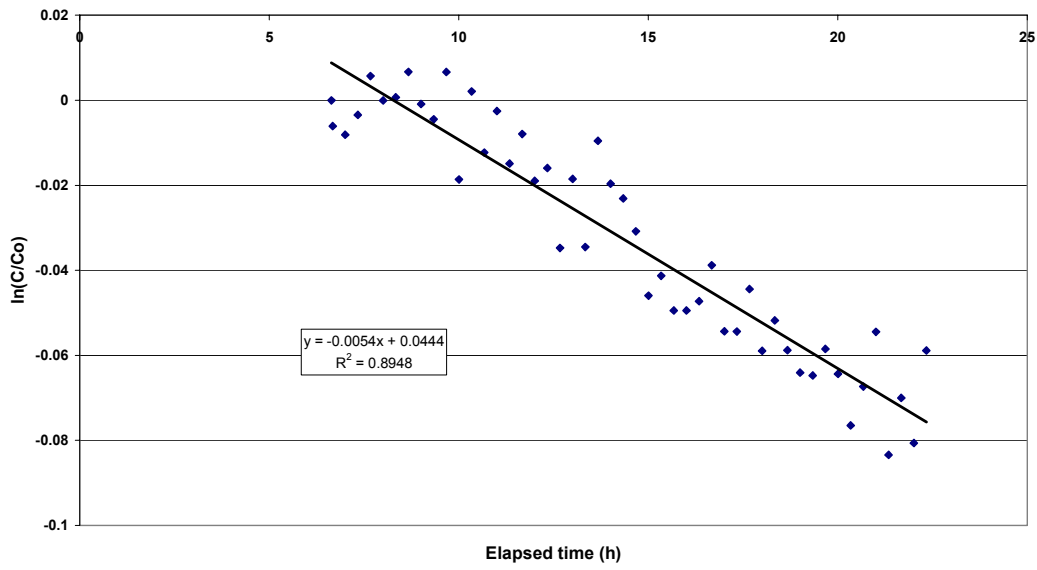
KLX02 338.4 - 341.4 m



KLX02 338.4 - 341.4 m



KLX02, 338.4-341.4 m



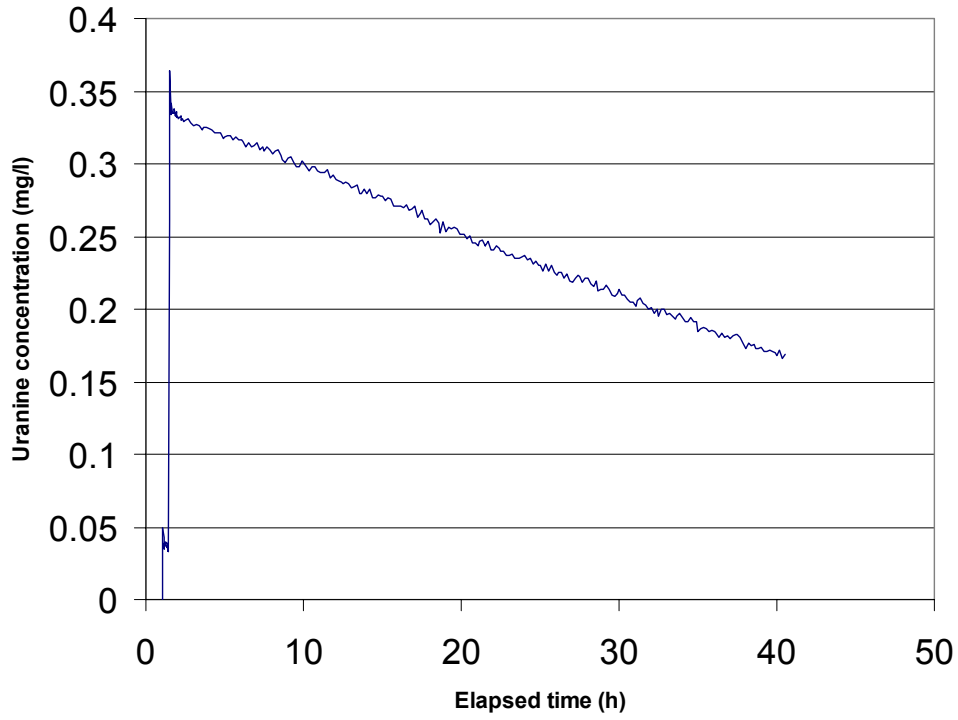
Part of dilution curve (h)	V (ml)	$\ln(C/C_0)/t$	Q (ml/h)	Q (ml/min)	Q (m ³ /s)	R2-value
7-22	4,645	-0.0054	25.08	0.42	6.97E-09	0.8948

Part of dilution curve (h)	K (m/s)	Q (m ³ /s)	A (m ²)	v (m/s)	l
7-22	2.00E-07	6.97E-09	0.454	1.54E-08	7.68E-02

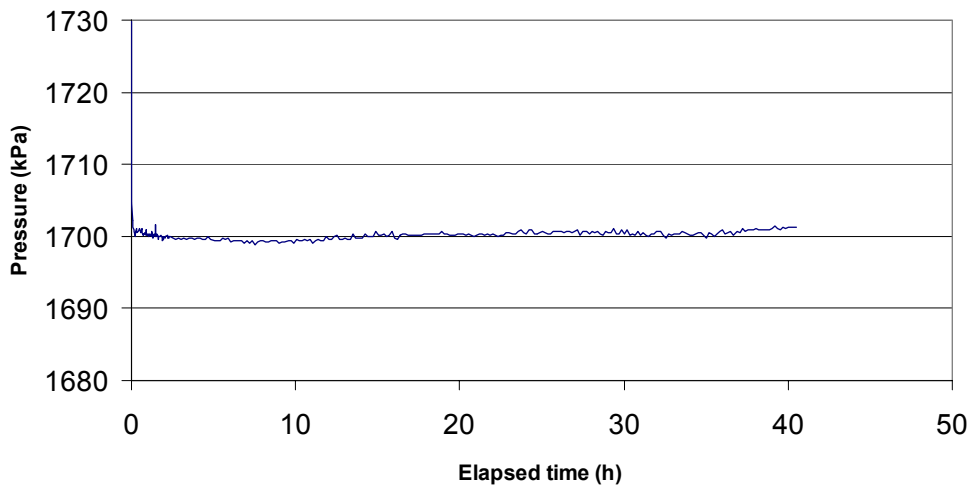
Dilution measurement KSH02

Dilution measurement KSH02 176.0–177.0 m

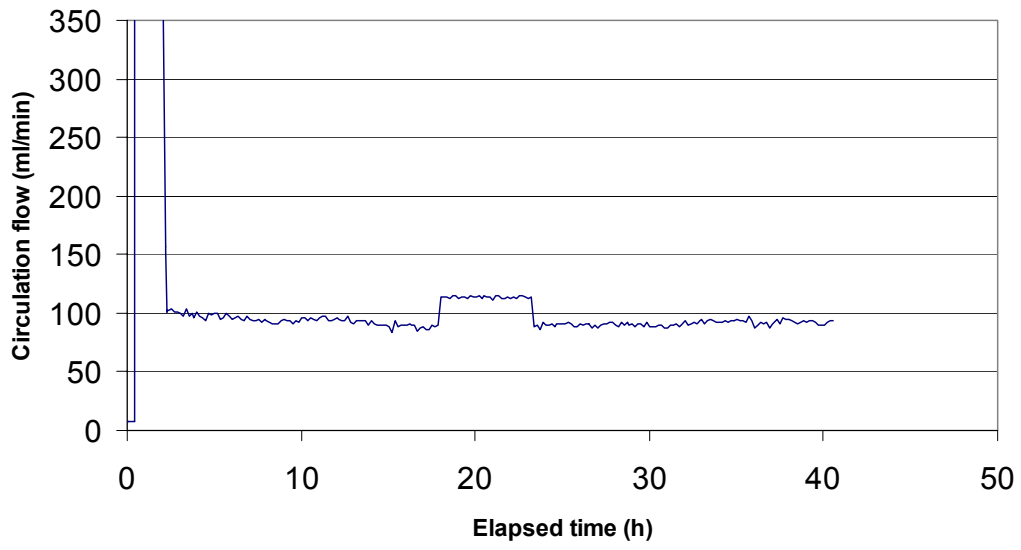
KSH02 176.0 - 177.0 m



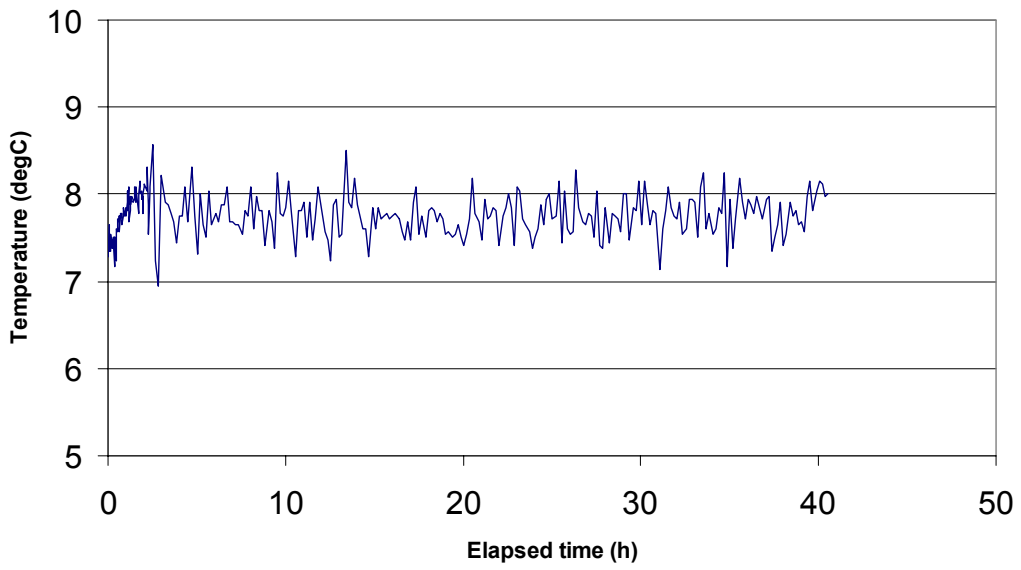
KSH02 176.0 - 177.0 m



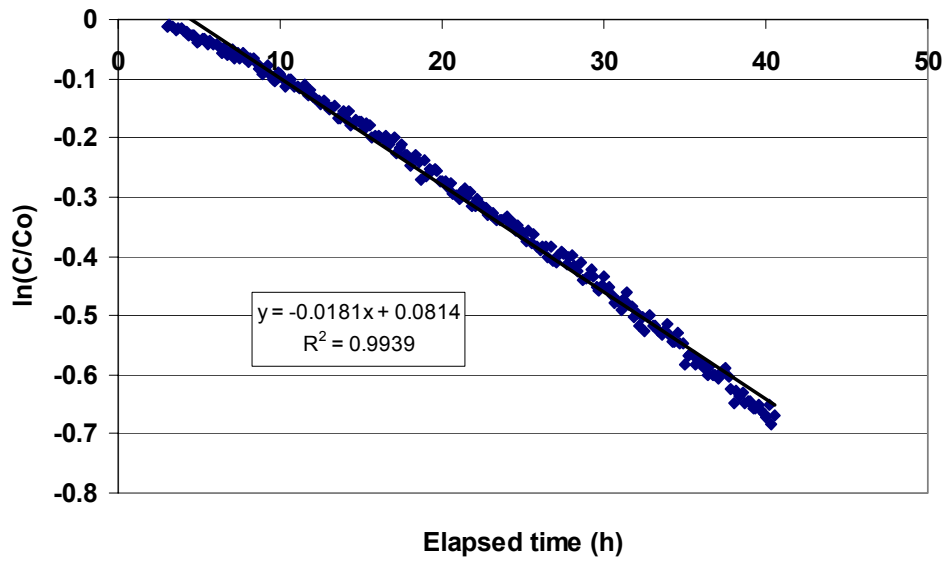
KSH02 176.0 - 177.0 m



KSH02 176.0 - 177.0 m



KSH02 176.0 - 177.0 m

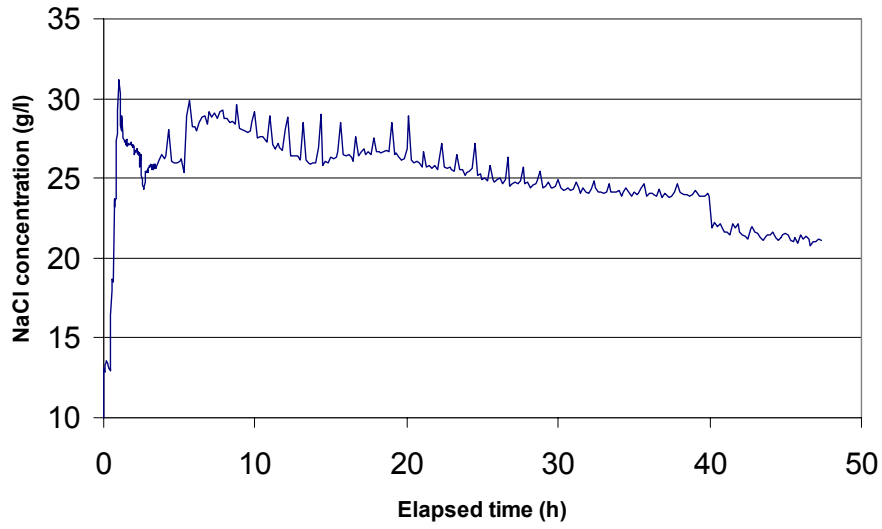


Part of dilution curve (h)	V (ml)	$\ln(C/Co)/t$	Q (ml/h)	Q (ml/min)	Q (m ³ /s)	R2-value
3-40	2,163	-0.0181	39.15	0.65	1.09E-08	0.9939

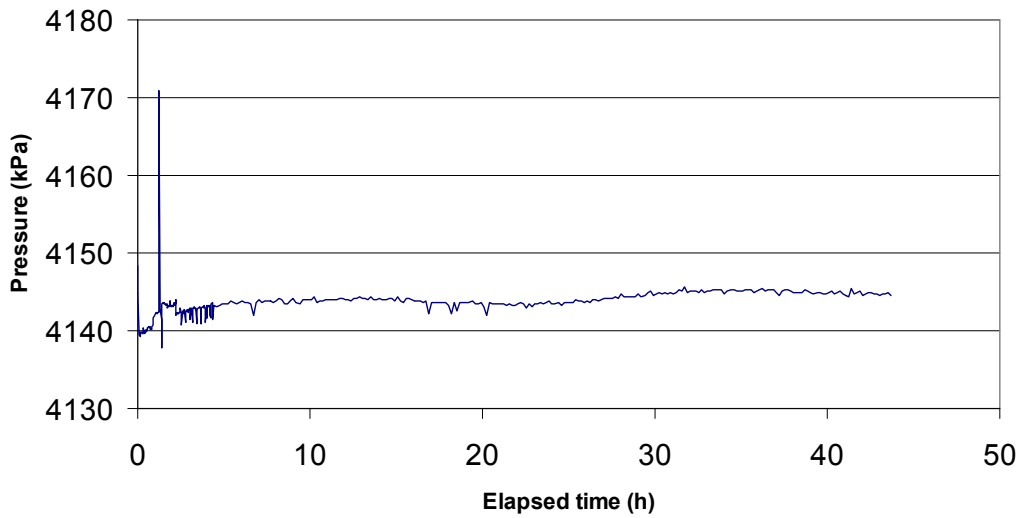
Part of dilution curve (h)	K (m/s)	Q (m ³ /s)	A (m ²)	v (m/s)	l
3-40	2.07E-07	1.09E-08	0.1514	7.18E-08	3.47E-01

Dilution measurement KSH02 422.3–423.3 m

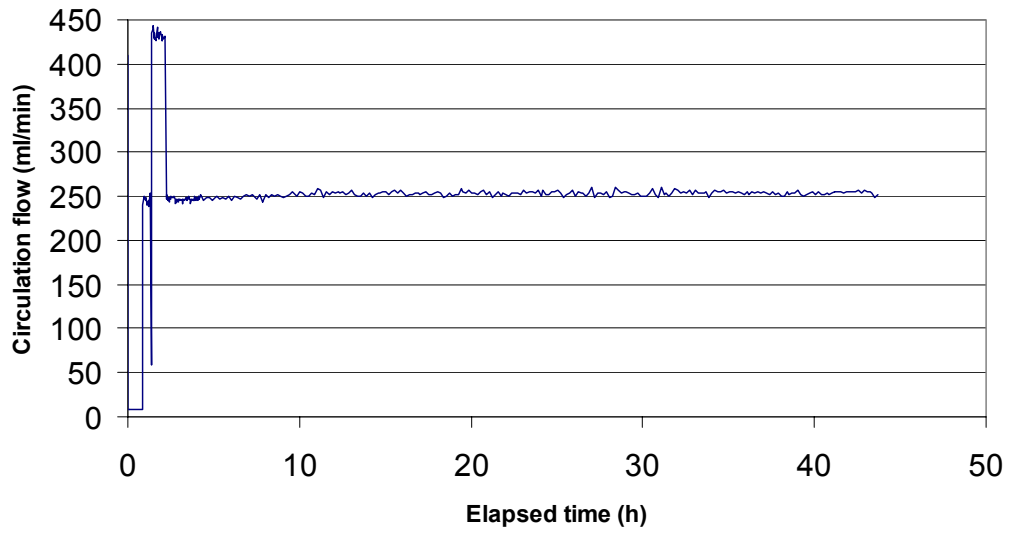
KSH02 422.3 - 423.3 m



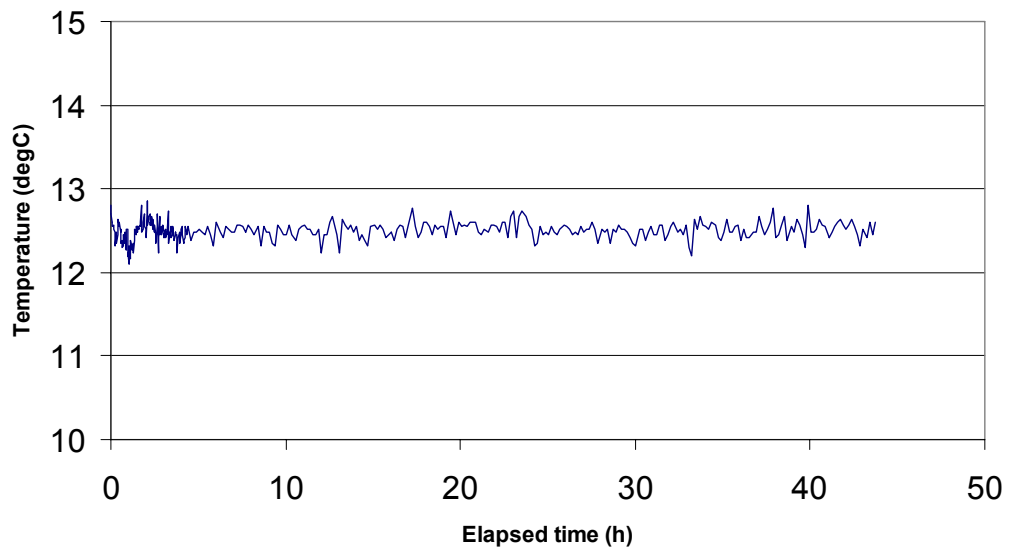
KSH02 422.3 - 423.3 m



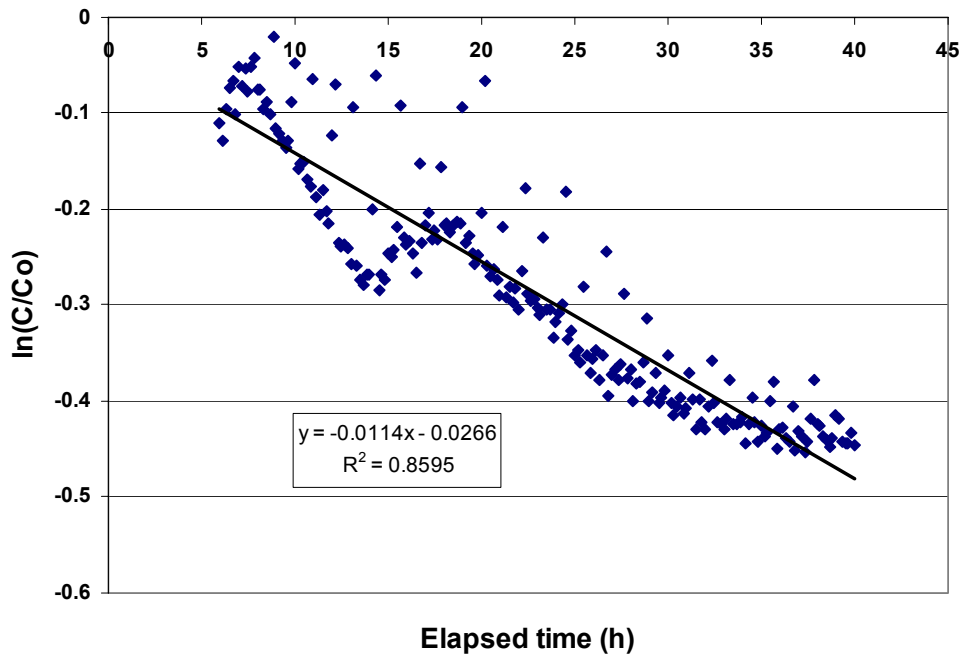
KSH02 422.3 - 423.3 m



KSH02 422.3 - 423.3 m



KSH02 422.3 - 423.3 m

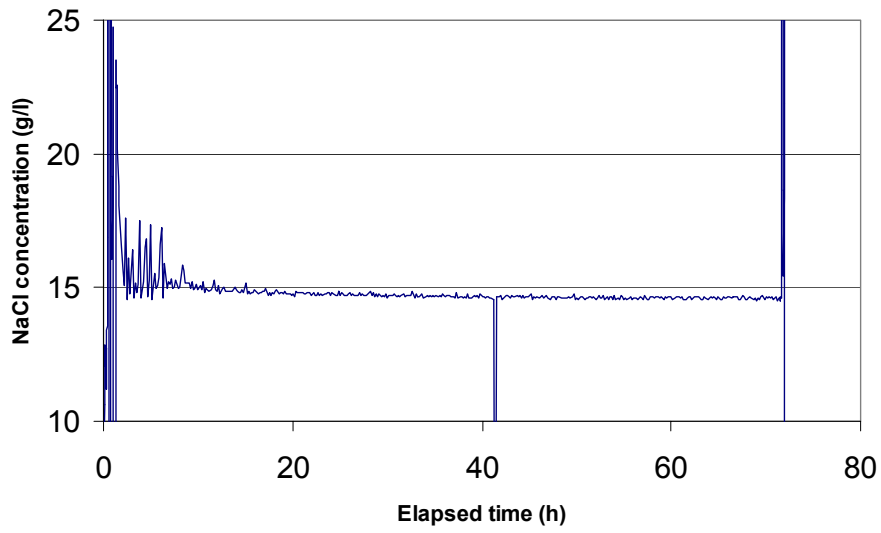


Part of dilution curve (h)	V (ml)	$\ln(C/C_0)/t$	Q (ml/h)	Q (ml/min)	Q (m ³ /s)	R2-value
6-40	1,026	-0.0114	11.70	0.19	3.25E-09	0.8595

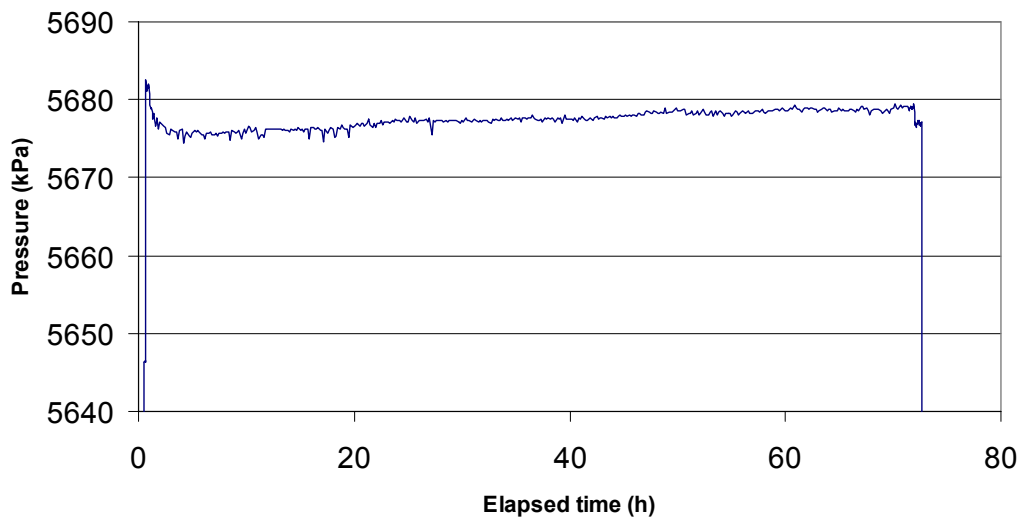
Part of dilution curve (h)	K (m/s)	Q (m ³ /s)	A (m ²)	v (m/s)	l
6-40	1.03E-06	3.25E-09	0.1514	2.15E-08	2.08E-02

Dilution measurement KSH02 576.8–579.8 m

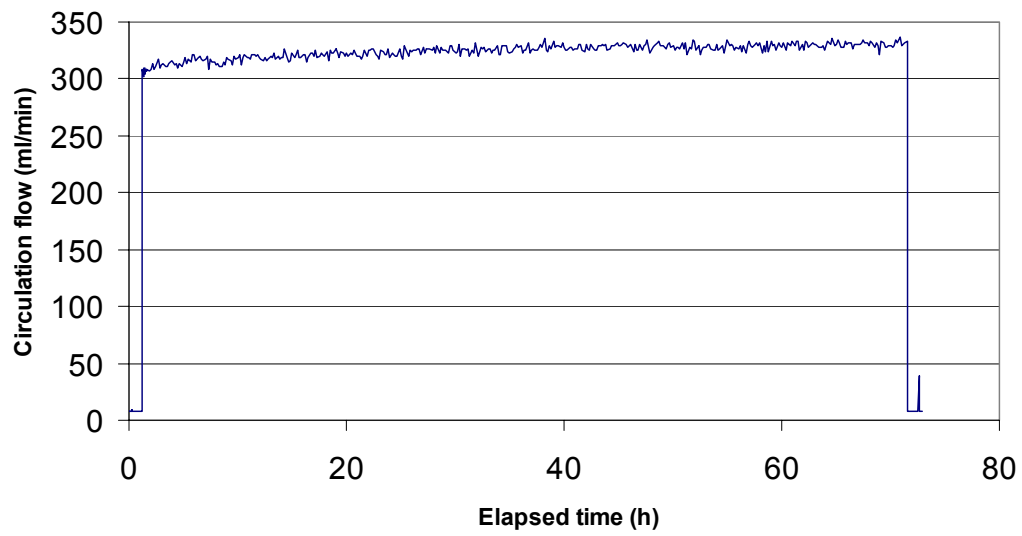
KSH02 576.8 - 579.8 m



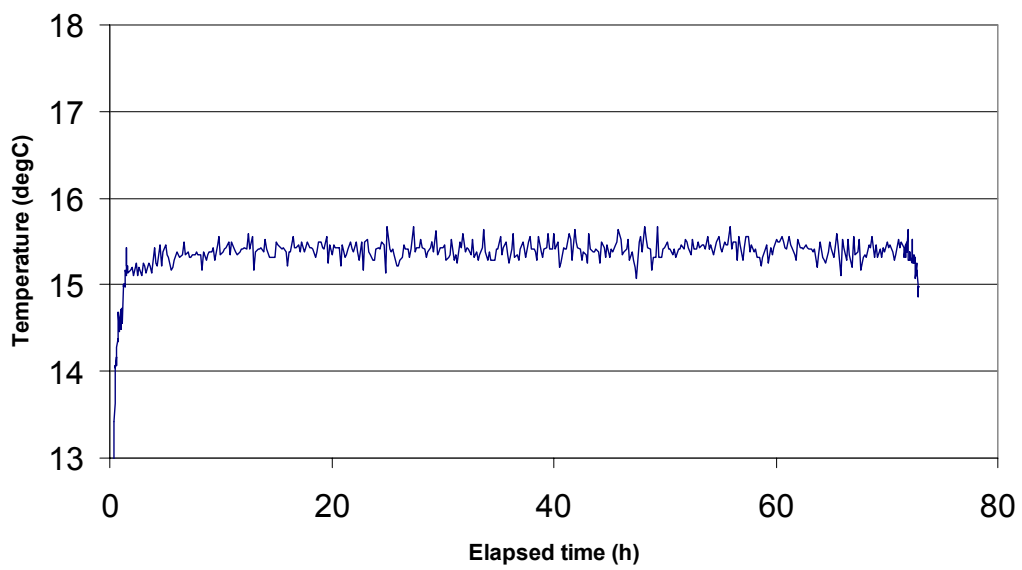
KSH02 576.8 - 579.8 m



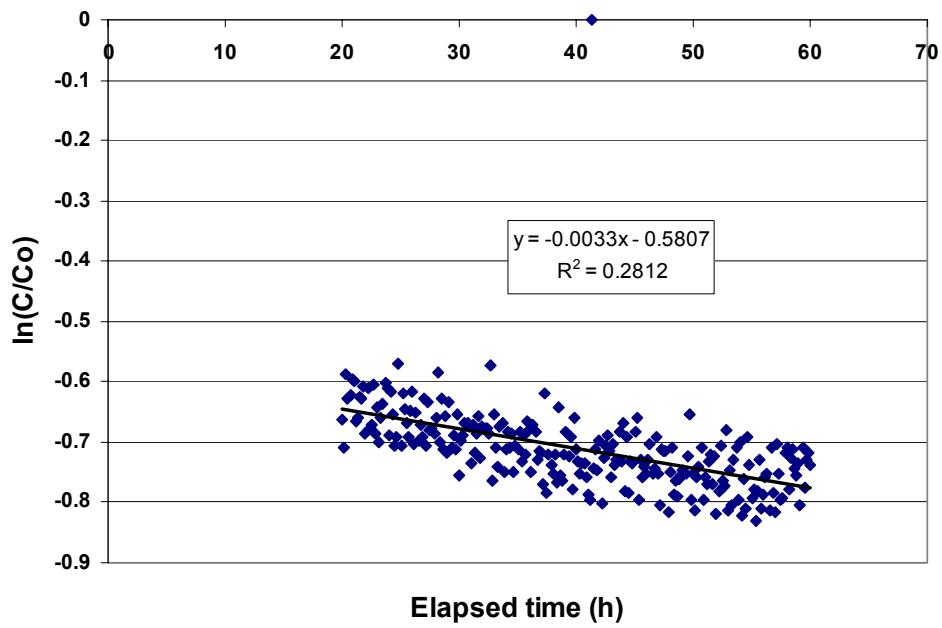
KSH02 576.8 - 579.8 m



KSH02 576.8 - 579.8 m



KSH02 576.8 - 579.8 m

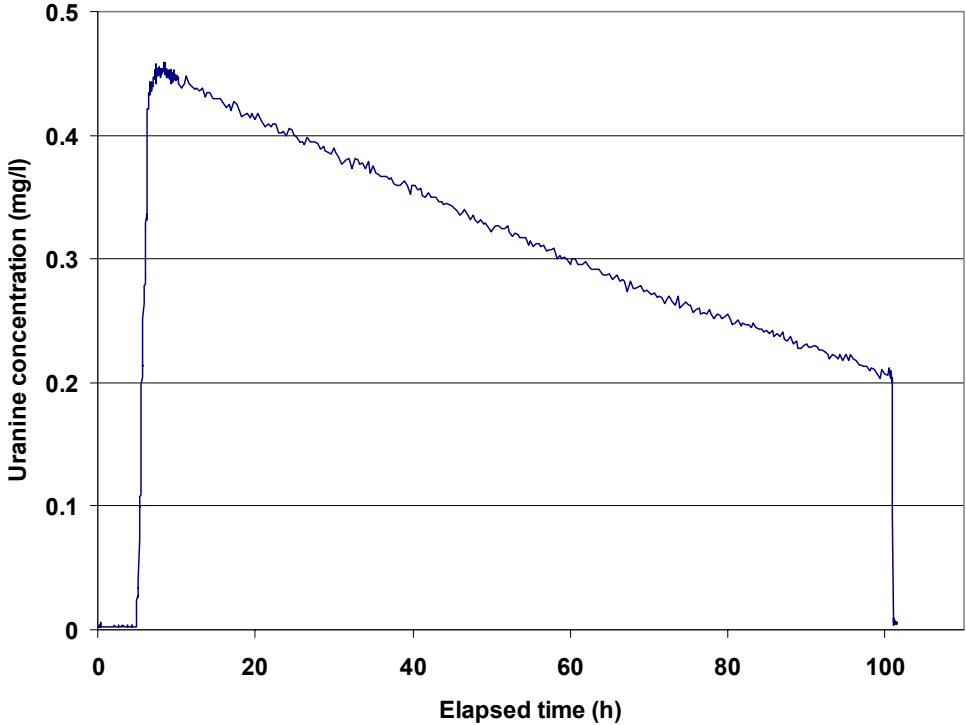


Part of dilution curve (h)	V (ml)	$\ln(C/Co)/t$	Q (ml/h)	Q (ml/min)	Q (m ³ /s)	R2-value
20.00–60.00	1,713	-0.0033	5.65	0.09	1.57E-09	0.2812

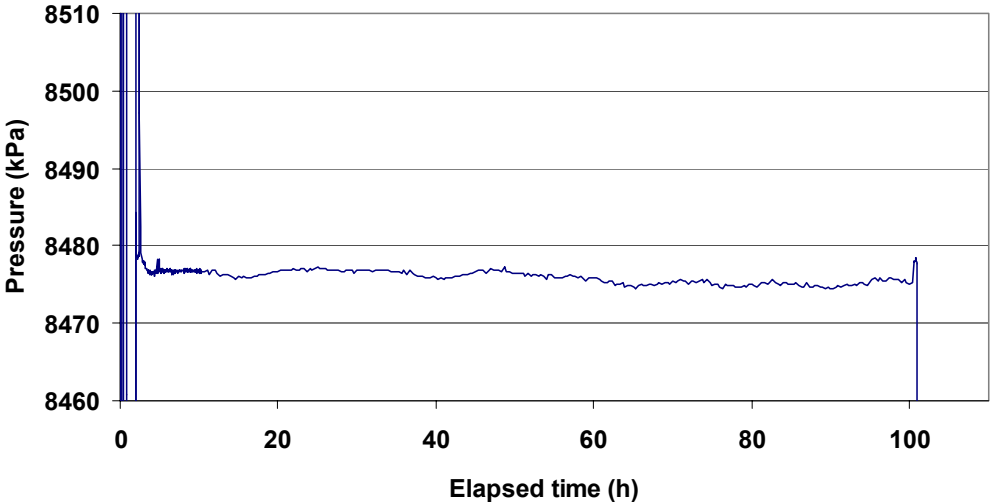
Part of dilution curve (h)	K (m/s)	Q (m ³ /s)	A (m ²)	v (m/s)	l
20.00–60.00	1.72E-07	1.57E-09	0.456	3.44E-09	2.00E-02

Dilution measurement KSH02 858.6–859.6 m

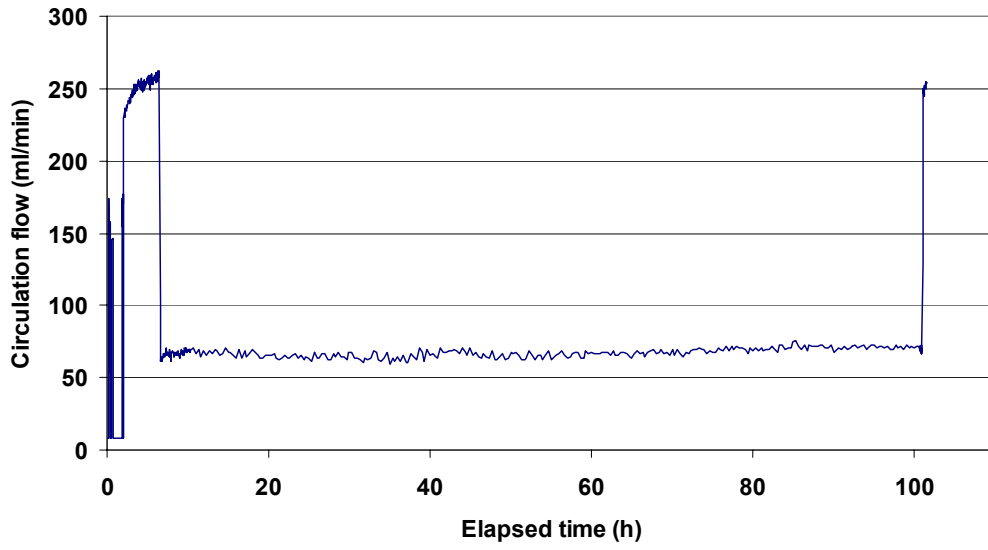
KSH02 858.6 - 859.6 m



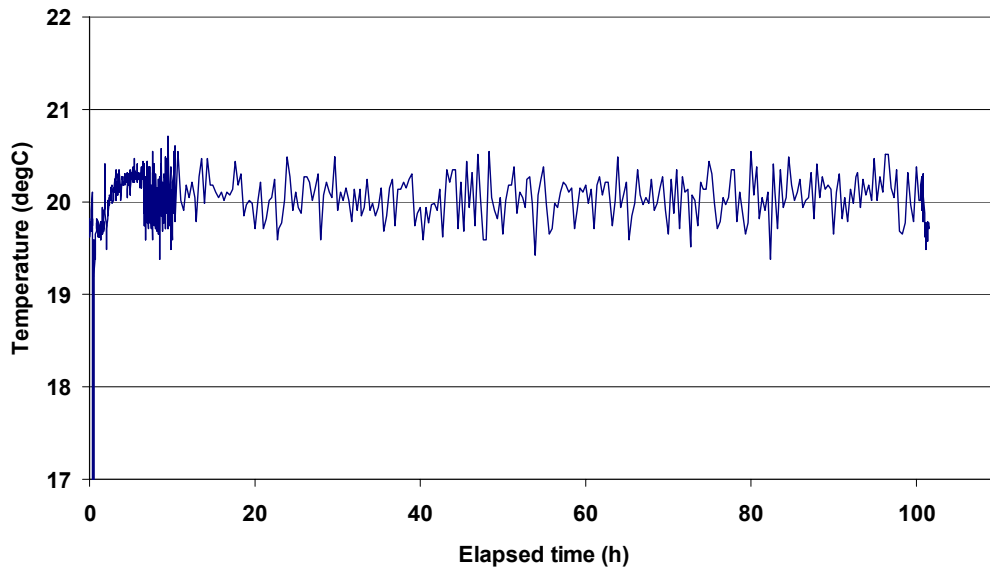
KSH02 858,6 - 859,6 m



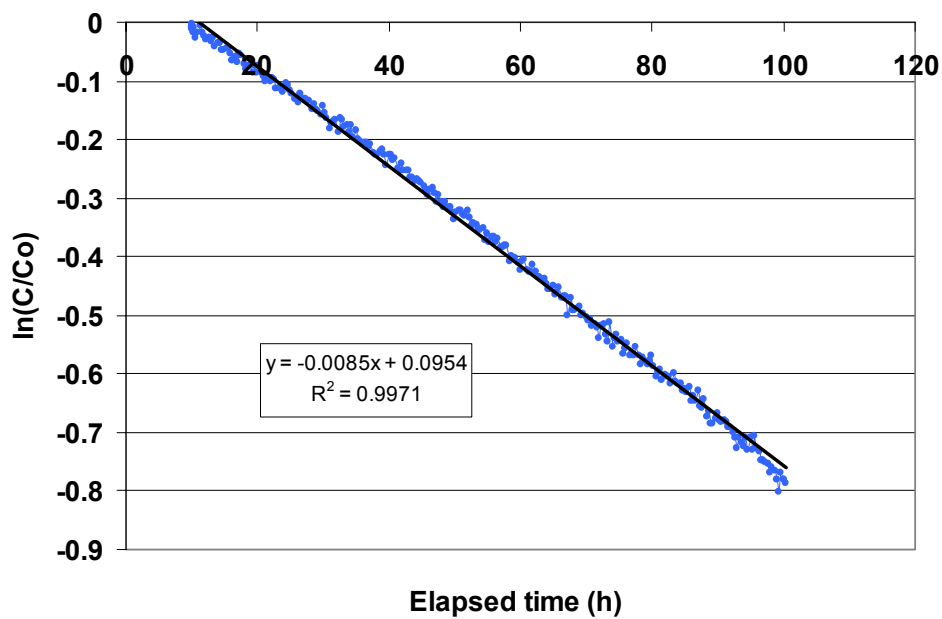
KSH02 858.6 - 859.6 m



KSH02 858.6 - 859.6 m



KSH02 858.6 - 859.6 m

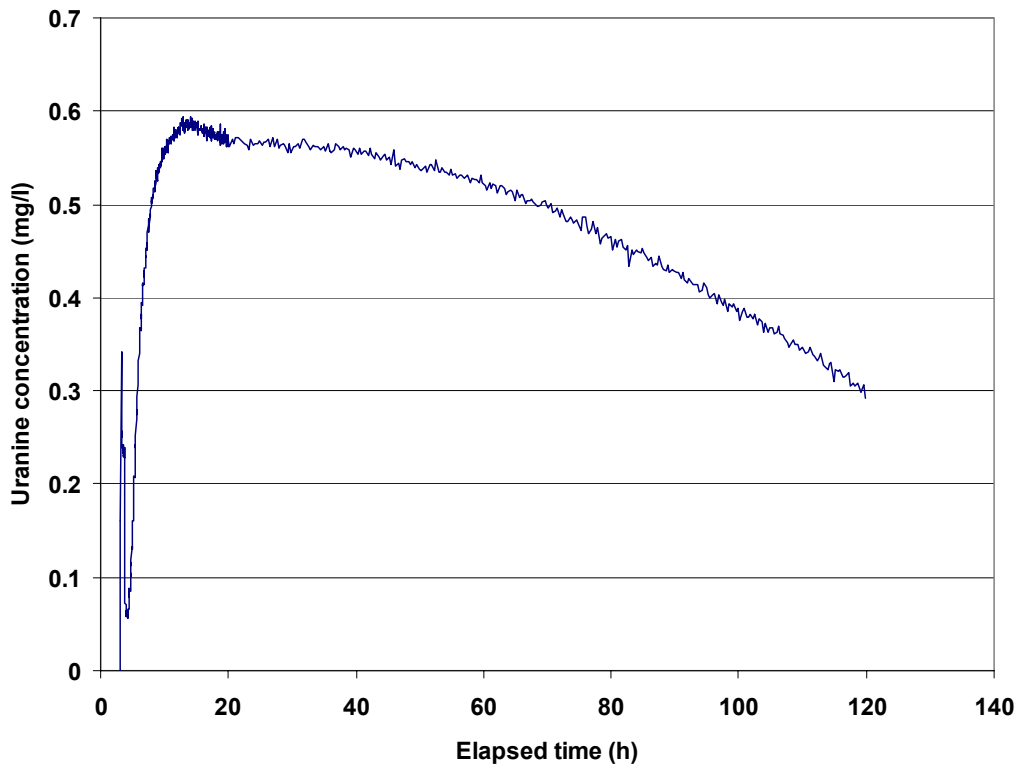


Part of dilution curve (h)	V (ml)	$\ln(C/C_0)/t$	Q (ml/h)	Q (ml/min)	Q (m ³ /s)	R2-value
10-100	2,163	-0.0085	18.39	0.31	5.17E-09	0.997

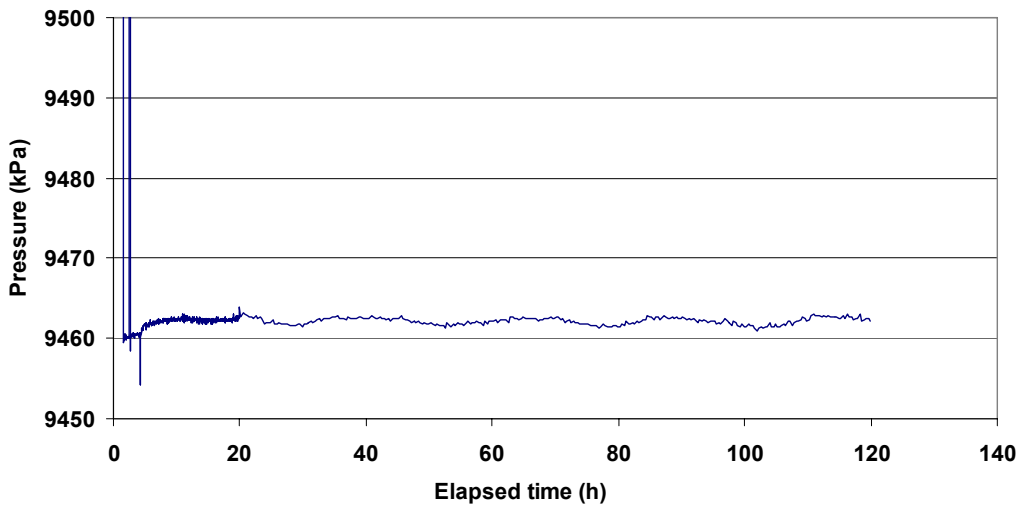
Part of dilution curve (h)	K (m/s)	Q (m ³ /s)	A (m ²)	v (m/s)	l
10-100	1.33E-08	5.17E-09	0.1514	3.41E-08	2,57E+00

Dilution measurement KSH02 957.2–958.2 m

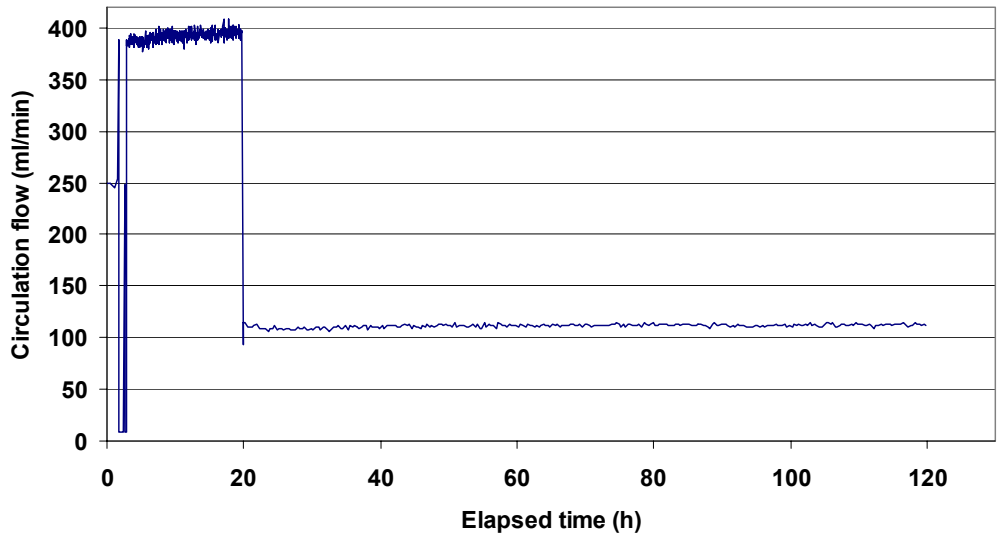
KSH02 957.2 - 958.2 m



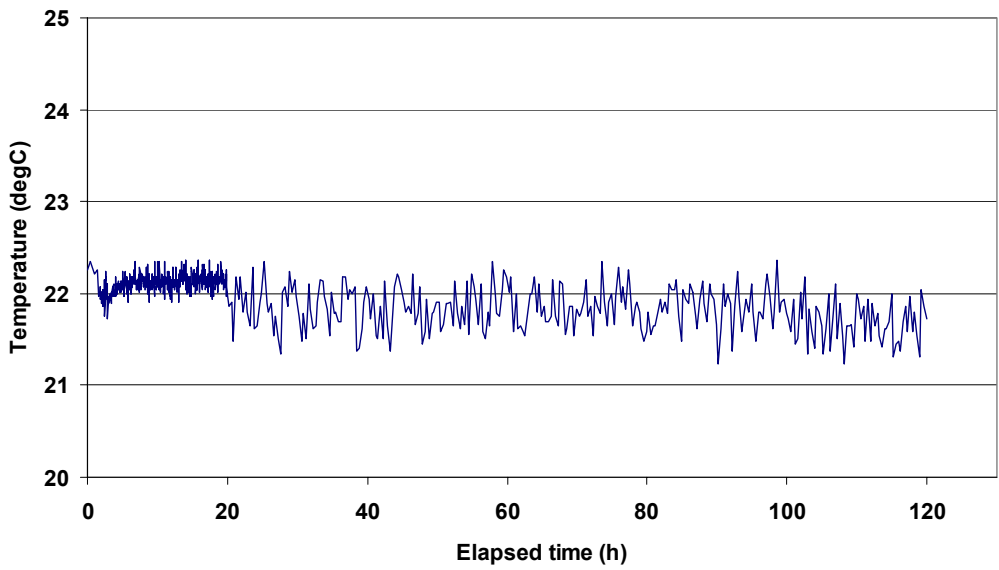
KSH02 957.2 - 958.2 m



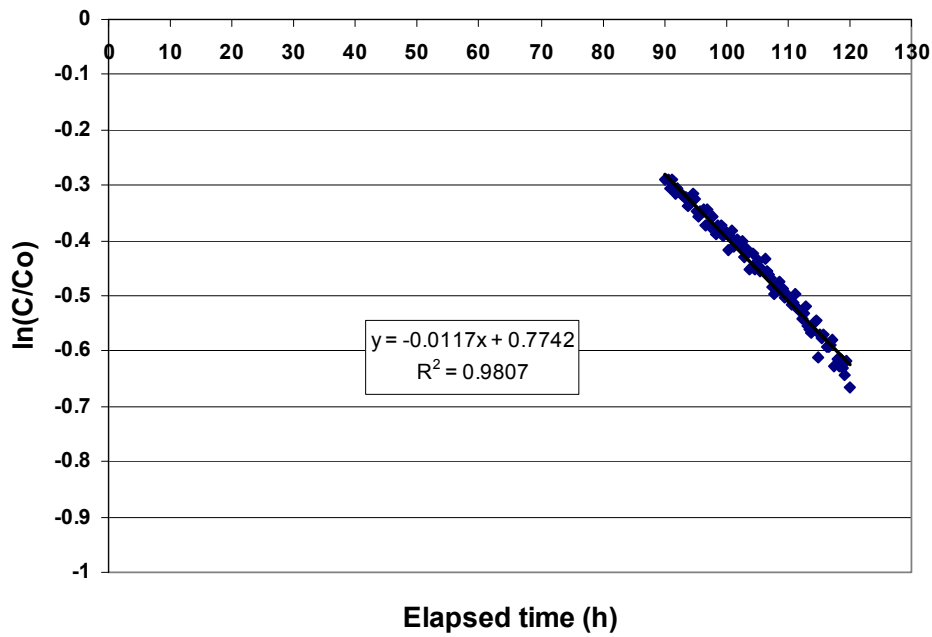
KSH02 957.2 - 958.2 m



KSH02 957.2 - 958.2 m



KSH02 957.2 - 958.2 m



Part of dilution curve (h)	V (ml)	ln(C/Co)/t	Q (ml/h)	Q (ml/min)	Q (m ³ /s)	R2-value
90-120	2,163	-0.0117	25.31	0.42	7.03E-09	0.981

Part of dilution curve (h)	K (m/s)	Q (m ³ /s)	A (m ²)	v (m/s)	l
90-120	5.38E-07	7.03E-09	0.1514	4.64E-08	8.63E-02